

Journal Pre-proof

Substituted 1-methyl-4-phenylpyrrolidin-2-ones – Fragment-based design of N-methylpyrrolidone-derived bromodomain inhibitors

J.P. Hilton-Proctor, O. Ilyichova, Z. Zheng, I.G. Jennings, R.W. Johnstone, J. Shortt, S.J. Mountford, M.J. Scanlon, P.E. Thompson



PII: S0223-5234(20)30087-8

DOI: <https://doi.org/10.1016/j.ejmech.2020.112120>

Reference: EJMECH 112120

To appear in: *European Journal of Medicinal Chemistry*

Received Date: 5 December 2019

Revised Date: 16 January 2020

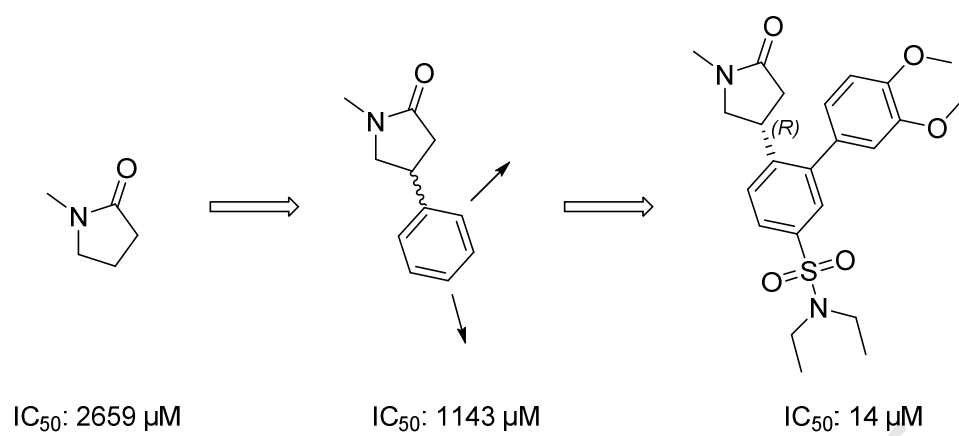
Accepted Date: 3 February 2020

Please cite this article as: J.P. Hilton-Proctor, O. Ilyichova, Z. Zheng, I.G. Jennings, R.W. Johnstone, J. Shortt, S.J. Mountford, M.J. Scanlon, P.E. Thompson, Substituted 1-methyl-4-phenylpyrrolidin-2-ones – Fragment-based design of N-methylpyrrolidone-derived bromodomain inhibitors, *European Journal of Medicinal Chemistry* (2020), doi: <https://doi.org/10.1016/j.ejmech.2020.112120>.

This is a PDF file of an article that has undergone enhancements after acceptance, such as the addition of a cover page and metadata, and formatting for readability, but it is not yet the definitive version of record. This version will undergo additional copyediting, typesetting and review before it is published in its final form, but we are providing this version to give early visibility of the article. Please note that, during the production process, errors may be discovered which could affect the content, and all legal disclaimers that apply to the journal pertain.

© 2020 Published by Elsevier Masson SAS.

Graphical abstract



Journal Pre-proof

Substituted 1-methyl-4-phenylpyrrolidin-2-ones – Fragment-Based Design of N-Methylpyrrolidone-Derived Bromodomain Inhibitors

Authors

Hilton-Proctor JP,¹ Ilyichova O,¹ Noor A,¹ Zheng Z,¹ Jennings IG,¹ Johnstone RW,^{2,3} Shortt J,^{4,5} Mountford SJ,¹ Scanlon MJ,¹ Thompson PE¹

Addresses

¹Medicinal Chemistry, Monash Institute of Pharmaceutical Science, Monash University, 381 Royal Parade, Parkville, Victoria, Australia

²Peter MacCallum Cancer Centre, 305 Grattan Street, Melbourne, Victoria, Australia

³The Sir Peter MacCallum Department of Oncology, University of Melbourne, Parkville, Victoria, Australia

⁴Blood Cancer Therapeutics Laboratory, School of Clinical Sciences at Monash Health, Monash University, 246 Clayton Road, Clayton, Victoria, Australia

⁵Monash Haematology, Monash Health, 246 Clayton Road, Clayton, Victoria, Australia

Keywords

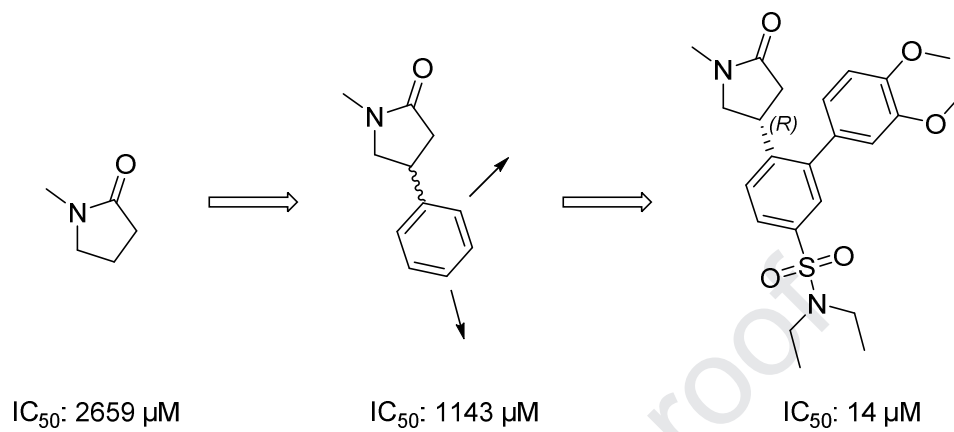
BRD4, Bromodomain, Epigenetics, K-ac, NMP

Abbreviations

BET, Bromodomain and Extra Terminal; BRD4 BD1, First Bromodomain of Bromodomain-containing Protein 4; FBDD, Fragment-based Drug Design; HPLC, High Performance Liquid Chromatography; K-ac, Acetyl-lysine; LLE, Lipophilic Ligand Efficiency; NHA, Non-

Hydrogen Atom; NMP, *N*-Methylpyrrolidone; RMS, Root Mean Square; SAR, Structure-Activity Relationship; vdW, van der Waals.

Graphical abstract



Abstract

N-Methylpyrrolidone is one of several chemotypes that have been described as a mimetic of acetyl-lysine in the development of bromodomain inhibitors. In this paper, we describe the synthesis of a 4-phenyl substituted analogue – 1-methyl-4-phenylpyrrolidin-2-one – and the use of aryl substitution reactions as a divergent route for derivatives. Ultimately, this has led to structurally complex, chiral compounds with progressively improved affinity as inhibitors of bromodomain-containing protein 4.

1. Introduction

Fragment-based drug design (FBDD) is a molecular design strategy that has gained significant traction as a means to develop new drug candidates.[1, 2] It fundamentally enacts a process of “growing” a small molecule with weak, but ligand efficient interactions with a target macromolecule into a high-affinity drug-like molecule. That growth is typically achieved by identifying a set of vectors and using functional group manipulations to extend away from the fragment to gain new interactions and thus improve binding affinity.[3-5]

In practice, the nature of the FBDD process has shown a tendency towards extended structures as the functional group transformations are based around building block chemistry.[6, 7] Obtaining more compact structures demands accessing multiple functional groups for elaboration on the same core fragment. There has also been a tendency to avoid chirality in fragment sets as it can lead to more complex syntheses.[8] However, recent efforts have embraced the discovery, synthesis and elaboration of racemic and chiral fragments to generate libraries and inhibitors.[9-15]

In our work, we wanted to consider both of these features as they might contribute towards compounds with increased novelty and characteristics such as structural rigidity that might provide for improved target affinity. Here, we report on the elaboration by successive aryl

substitution of 1-methyl-4-phenylpyrrolidin-2-one, a chiral, phenyl-substituted version of the solvent *N*-methylpyrrolidone (NMP) as a bromodomain and extra terminal (BET) bromodomain inhibitor.

Despite the vast amount of effort that has gone into elaborating the many fragments that are known to fit inside the acetyl-lysine (K-ac) binding site,[14, 16-22] NMP has been neglected in these efforts. NMP's historic use has been in industrial applications such as paint removal and coatings, along with pharmaceutical purposes including drug solubilisation[23] and depot injections, remarked for its low reactivity and toxicity. NMP has affinity for several bromodomains[24] and crystallographic work has established that NMP fits into the conserved areas of the K-ac binding pocket. NMP shows antimyeloma and immunomodulatory activity in multiple myeloma models, which is attributed to pleiotropic bromodomain inhibition.[25] At the moment, it is in a phase I clinical trial for the treatment of multiple myeloma.[26] NMP also has a well-documented history with bone diseases like rheumatoid arthritis and osteoporosis[27] by preventing bone resorption[28] and fat accumulation in bone marrow.[29]

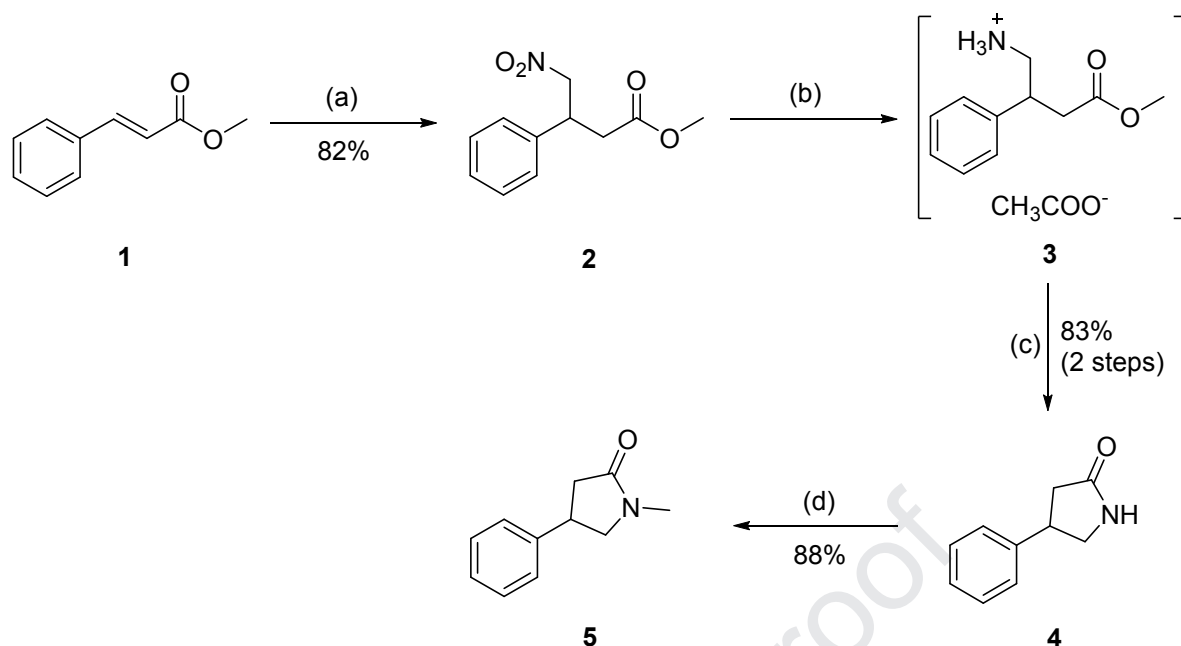
NMP has also served as the inspiration in the development of other novel mimetic warheads, including the dimethylisoxazole[16] and dihydroquinazolinone.[30] Both of these mimetics have been greatly utilised in the development of clinical inhibitors[31] and probes.[21, 32, 33] We recently described the elaboration of the NMP structure with a series of aliphatic extensions, which include preparing a mimic of the acetamide-containing bromodomain inhibitor, Olinone.[34] In this manuscript, we describe the efforts undertaken to develop aryl-functionalised derivatives of NMP as inhibitors of the first bromodomain of bromodomain-containing protein 4 (BRD4 BD1).

2. Results and Discussion

Based upon the available crystal structures of NMP (Supplementary Video S1), we decided that the 4-position would be the most appropriate place to substitute a phenyl ring, which is a suitable group to further functionalise through electrophilic aromatic substitution reactions. Substituted analogues have the potential to interact with the ZA channel and WPF shelf regions of the bromodomain binding pocket in a similar manner to other inhibitors reported previously.[21, 31, 32]

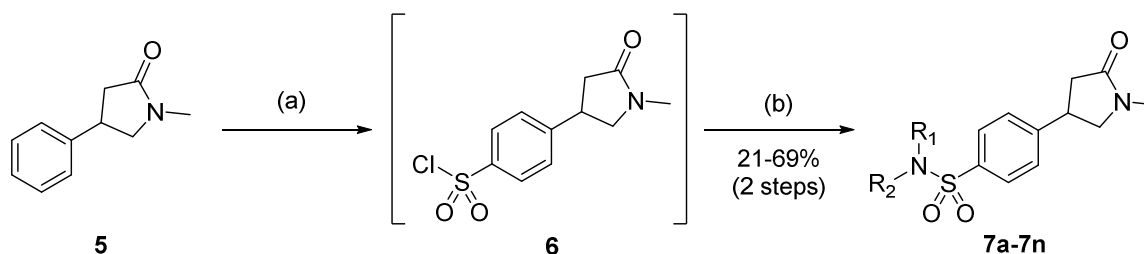
2.1. Synthesis

The scheme for preparing 1-methyl-4-phenylpyrrolidin-2-one **5** is outlined in Scheme 1. Commercially-available methyl *trans*-cinnamate **1** was reacted with nitromethane and 1,1,3,3-tetramethylguanidine via Michael addition to afford the nitroester **2** in 82% yield as previously reported[35]. The reduction of **2** to the amine **3** and then cyclisation to the lactam **4** was achieved by hydrogenation with acetic acid as the solvent. Reduction under these conditions gave the amine **3** as an acetate salt. Refluxing **3** in a mixture of ethanol and triethylamine drove cyclisation of **3** to the lactam **4** in good yields across the 2 steps. The lactam was then methylated by methyl iodide and sodium hydride to give the desired phenyl NMP derivative **5**. [36] This procedure reliably gave **5** on gram scale with 50% overall yield.



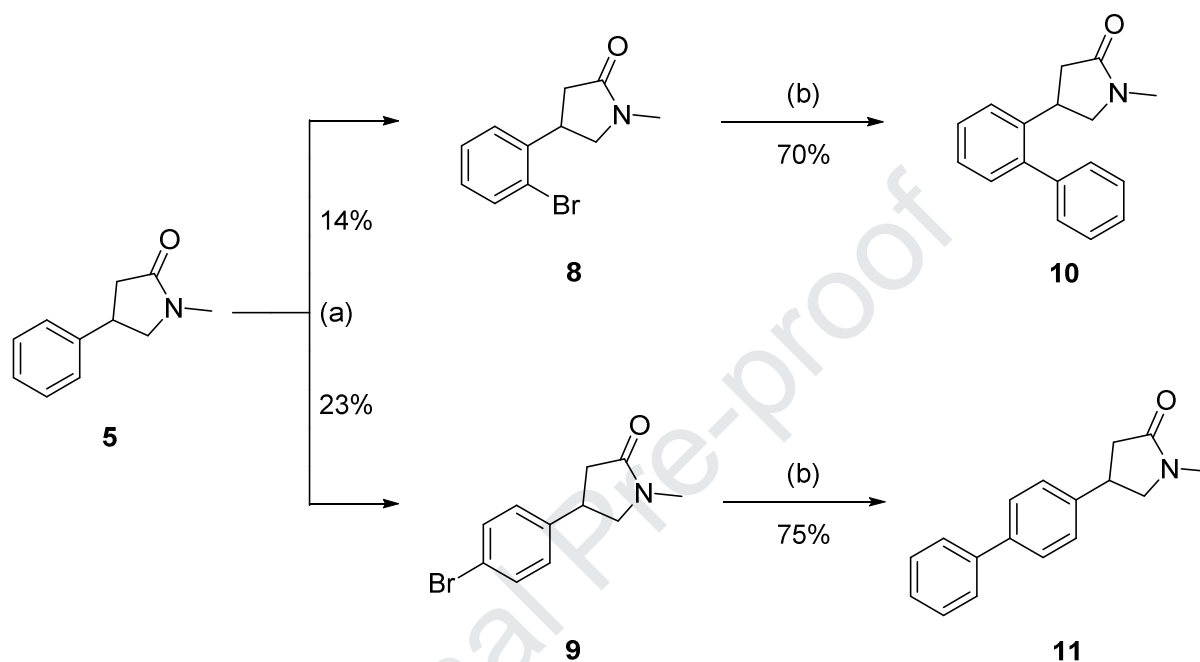
Scheme 1. Synthesis of **5**. Reagents and conditions: (a): CH_3NO_2 , 1,1,3,3-tetramethylguanidine, 42 h, rt; (b): H_2 , Pd/C, CH_3COOH , 4 d, rt; (c): Et_3N , EtOH, o/n, reflux; (d): N_2 , NaH, MeI, THF, o/n, $0^\circ\text{C} \rightarrow \text{rt}$.

With the core scaffold **5** in hand, the next step was to functionalise the phenyl group which was achieved with chlorosulfonation followed by amine substitution of the resultant sulfonyl chloride. Treatment of **5** with an excess of chlorosulfonic acid gave the intermediate **6**. The *para*-substituted sulfonyl chloride **6** was treated with a range of primary and secondary amines to generate sulfonamides **7a-7n** in yields ranging from 21-69% (Scheme 2).



Scheme 2. General formation of sulfonamides **7**. (a): ClSO_3H , CH_2Cl_2 , o/n, rt; (b): NR_1R_2 , Et_3N , CH_2Cl_2 , o/n, rt.

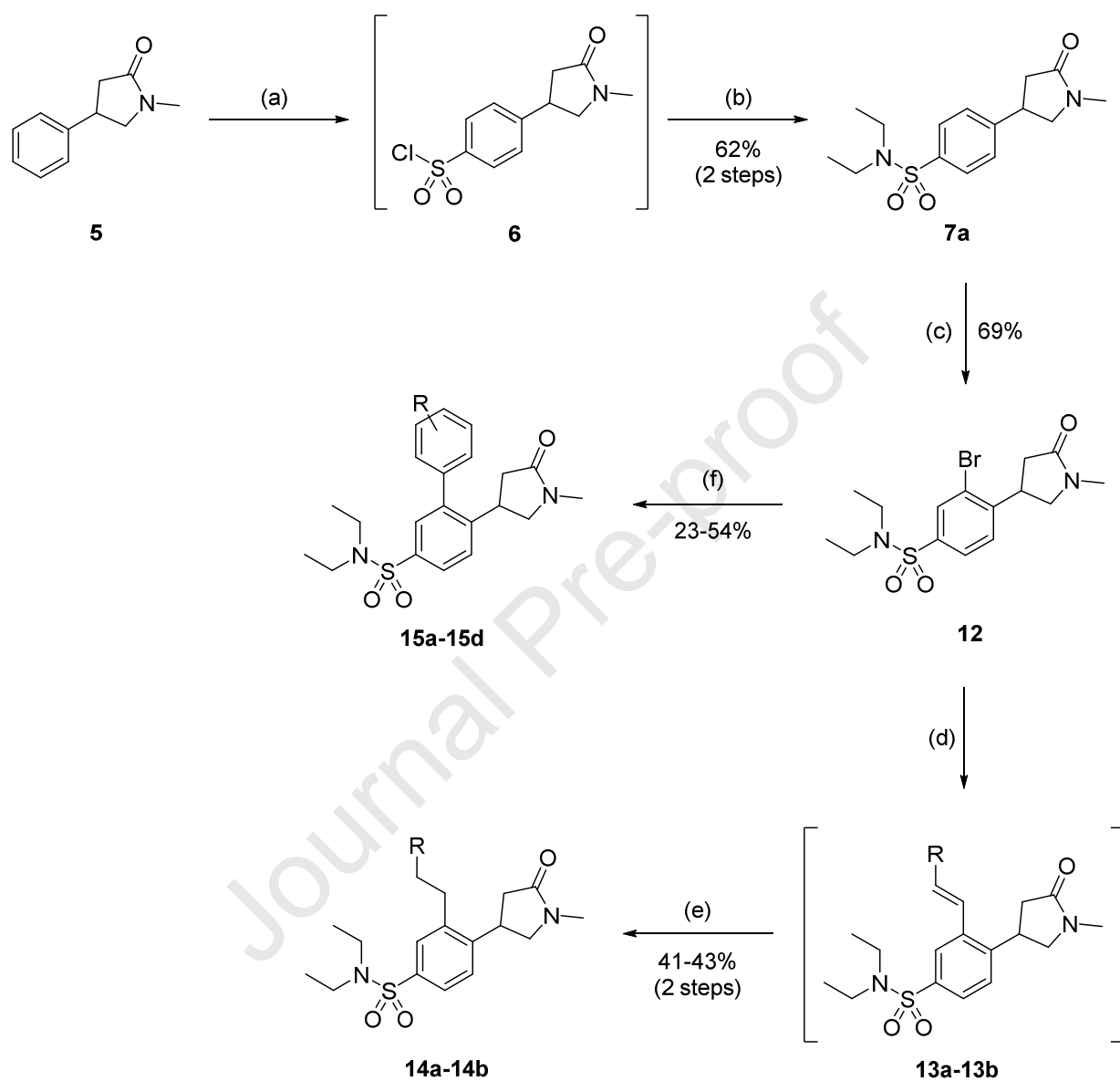
Alternatively, bromination using sodium bromide and sulfuric acid[37] gave a mixture of both *ortho*- (**8**) and *para*-substituted (**9**) products (Scheme 3) which were separated by column chromatography. These aryl bromides underwent Suzuki coupling with phenylboronic acid, giving the biphenyl NMP derivatives **10** and **11** in respectable yields.[38]



Scheme 3. Formation of bromides **8** and **9** with subsequent Suzuki coupling. (a): NaBr, H₂SO₄, 2 h, 80 °C. (b): N₂, PhB(OH)₂, Pd(PPh₃)₄, 1,2-dimethoxyethane, 2 M Na₂CO₃, 4 h, reflux.

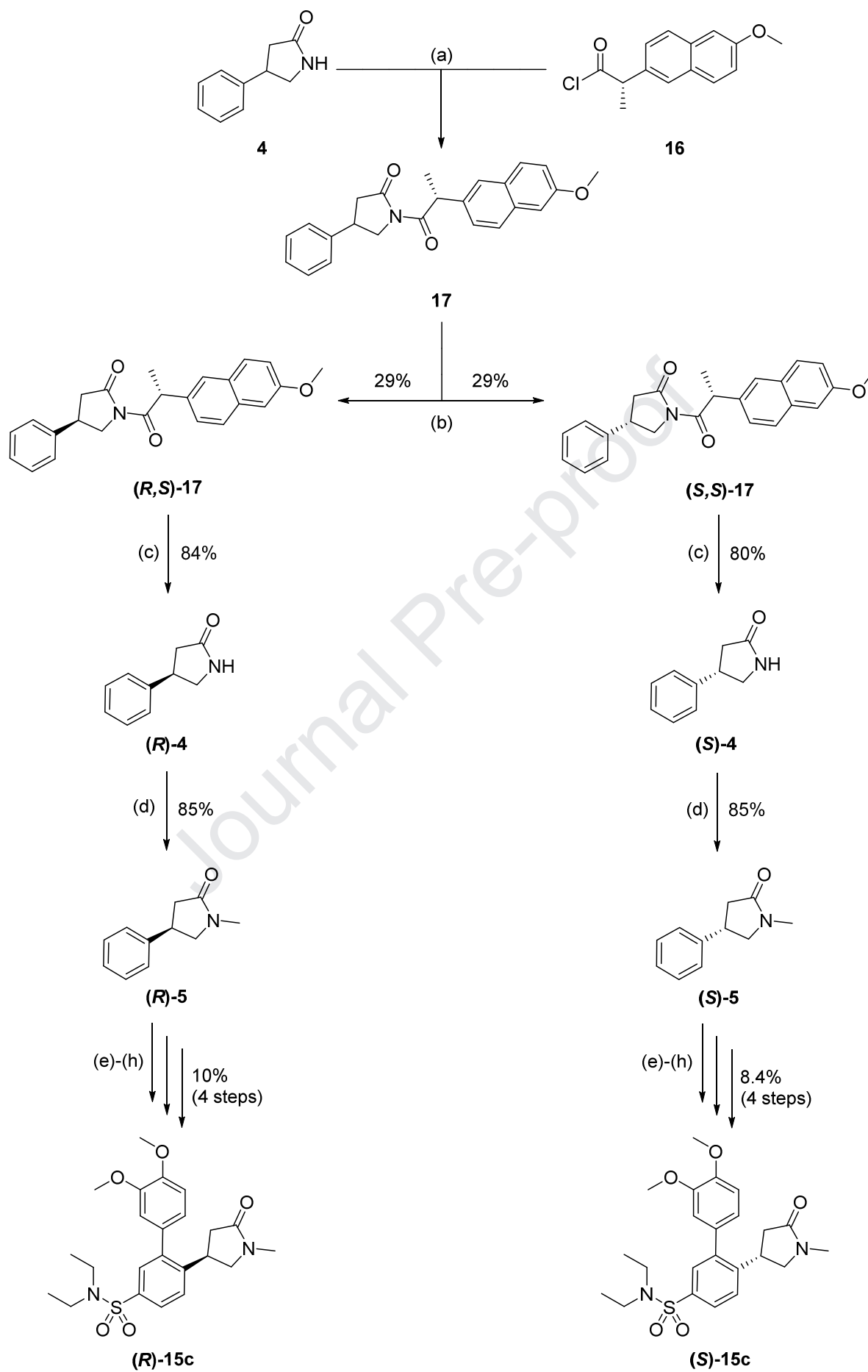
The alkyl sulfonamides showed promising affinity (discussed later), so the diethyl sulfonamide **7a** was used to further functionalise the aryl group via bromination to give tri-substituted benzene products. As outlined in Scheme 4, **7a** was treated with a mixture of *N*-bromosuccinimide and sulfuric acid to give **12** in good yield.[39] The aryl bromide **12** was then subject to cross-coupling reactions. Heck coupling gave a series of alkenes (**13**) which were in turn reduced to the corresponding alkanes (**14**). Suzuki coupling using the method described above gave a series of biaryl compounds (**15**).[40] The coupling of a thianaphthene group (**15d**) resulted in atropisomerism due to the hindered rotation between the

thianaphthene and NMP moieties. This was shown by the broadening of the NMP signals in the ^1H NMR, while the signals for the other compounds in this series were well-defined.



Scheme 4. Formation of sulfonamide **7a** with bromination and cross-coupling of **12**. (a): ClSO_3H , CH_2Cl_2 , o/n, rt; (b): Et_2NH , Et_3N , CH_2Cl_2 , o/n, rt. (c): NBS , H_2SO_4 , o/n, rt. (d): N_2 , R-alkene, $\text{P}(\text{o-tol})_3$, $\text{Pd}(\text{OAc})_2$, DIPEA , DMF , o/n, 90°C ; (e): H_2 , Pd/C , EtOAc , o/n, rt; (f): N_2 , R-B(OH) $_2$, $\text{Pd}(\text{PPh}_3)_4$, 1,2-dimethoxyethane, 2 M Na_2CO_3 , 4 h, reflux.

The chiral nature of all these products led us to examine the generation of single enantiomers of **5**, as well as the biaryl derivative **15c** by diastereomeric resolution. As shown in Scheme 5, lactam **4** was treated with lithium diisopropylamide and (*S*)-Naproxen chloride **16**[41] to give diastereomeric imides **17**, which were separated carefully by column chromatography to acquire the (*R,S*)-**17** and (*S,S*)-**17**. In agreement with the literature, the ¹H NMR signals of the first eluted product corresponded with the (*R,S*)-diastereomer, and the proton signals of the second product matched the (*S,S*)-diastereomer. The imides were hydrolysed with aqueous potassium hydroxide to give (*R*)-**4** and (*S*)-**4**. The specific rotation of each enantiomer was consistent with literature values. They were then methylated as above to give the respective isomers (*R*)-**5** and (*S*)-**5**, which were carried forward to (*R*)-**15c** and (*S*)-**15c** using the same conditions described as in Scheme 4. The enantiomers resolved well by chiral chromatography and matched the corresponding peaks in the racemic mixture, with the first eluting product being the *S*-enantiomer.



Scheme 5. Stereoisomer resolution of **4** with corresponding synthesis of phenyl NMP isomers. (a): LDA, THF, 3 h, $-78\text{ }^{\circ}\text{C}$. (b): Column chromatography, 10% EtOAc in petroleum benzene. (c): 1 M KOH, THF, o/n, rt. (d): NaH, MeI, THF, N_2 , o/n, $0\text{ }^{\circ}\text{C} \rightarrow \text{rt}$. (e): ClSO_3H , CH_2Cl_2 , o/n, rt; (f): Et_2NH , Et_3N , CH_2Cl_2 , o/n, rt. (g): NBS, H_2SO_4 , o/n, rt. (h): N_2 , $(\text{CH}_3\text{O})_2\text{-C}_6\text{H}_3\text{-B(OH)}_2$, $\text{Pd(PPh}_3)_4$, 1,2-dimethoxyethane, 2 M Na_2CO_3 , 4 h, reflux.

2.2. BRD4 BD1 FRET Assay Results

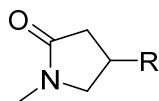
The phenyl-substituted NMP compounds were all assessed for inhibition of a biotinylated tetra-acetylated histone peptide ($\text{H4K}^5\text{K}^8\text{K}^{12}\text{K}^{16}(\text{ac}_4)$) binding to BRD4 BD1 in a FRET-based assay. The results of the first series of assays are shown in Table 1.

Firstly, the addition of a phenyl group to NMP (**5**) increased the binding affinity for BRD4 BD1 by approximately 2-fold. This confirmed the suitability of the aryl substituent for functionalisation of NMP.

Introduction of the sulfonamide group gave some significant improvements with alkyl sulfonamides **7a**, **7b**, **7h** and **7i** having IC_{50} values between 120 – 150 μM , nearly a 10-fold increase from **5**. However, other alterations to the sulfonamide – arylpiperidines, tetrahydroquinolines, benzylamines and nipecotic acids – resulted in a loss of activity. An interesting observation was that the activity of **7n** was similar to compounds **7a**, **7b**, **7h** and **7i**, despite possessing a bulky adamantyl group. These observations, paired with the generated X-ray crystal structures to be discussed later, suggest that certain aliphatic substituents are best tolerated.

The introduction of a bromine group resulted in improved affinity compared to **5**; the *ortho*-bromide **8** (321 μM) had marginally affinity than the *para*-bromide **9** (417 μM). The substitution to a phenyl group was also tolerated, but was preferable in the *para* position **11** (434 μM) compared to the *ortho* position **10** (575 μM).

Table 1. SAR data on initial phenyl NMP derivatives.



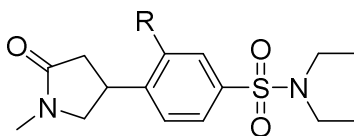
Compound Number	R=	IC ₅₀ (μM ± SEM) ^a	cLogP ^d	LLE ^e
	H	2660 ± 480	-0.40	2.97
5		1140 ± 10	1.16	1.78
7a		123 ± 29	1.08	2.83
7b		144 ± 18	1.55	2.29
7c		276 ± 12	0.30	3.26
7d		473 ± 13	2.96	0.37
7e		450 ± 33	2.48	0.87
7f		443 ^c	1.71	1.65
7g		250 ± 3 ^b	0.14	3.46
7h		147 ± 5 ^b	0.67	3.16
7i		134 ± 7 ^b	0.45	3.42
7j		223 ± 23 ^b	0.55	3.10
7k		1680 ± 240	0.76	2.01

Table 1 (continued).

7l		1960 ± 90	0.76	1.95
7m		1390 ± 20	0.19	2.67
7n		151 ± 43	2.60	1.22
8		321 ± 48	2.02	1.47
9		417 ± 25	2.02	1.36
10		575 ± 177	2.75	0.49
11		434 ± 116	3.05	0.31

^aUnless stated otherwise, all results of means are $n \geq 2$. ^bSD reported. ^c $n = 1$. ^dcLogP values were calculated using ChemDraw 18.1. ^eLipophilic ligand efficiency = $-\log(\text{IC}_{50}) - \text{cLogP}$. Control compound used: **I-BET726** (IC_{50} : 0.01 μM).

The synthetic elaboration of **7a** yielded di-substituted aryl NMP analogues that produced a range of activities, which are shown in Table 2. The addition of the bromide to the selected sulfonamide (**12**) resulted in a 5-fold poorer inhibitor compared to **7a**. The products from the Heck/hydrogenation steps (**14a** – **14b**) were found to be inactive. The change to a phenyl group (**15a**) was detrimental to activity, but compound **15c** showed much improved inhibition with an IC_{50} of 52 μM .

Table 2. SAR data on halide-coupled NMP derivatives from **7a**.

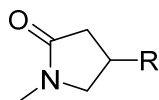
Compound Number	R=	IC ₅₀ (μM ± SEM) ^a	cLogP ^c	LLE ^d
7a	H	123 ± 29	1.08	2.83
12	Br	652 ± 116	1.95	1.24
14a		4500 ± 40	3.48	-1.13
14b		>5000	4.01	-1.70
15a		3200 ± 80	2.67	-0.18
15b		217 ± 19	2.90	0.77
15c		51.6 ± 2.5	2.35	1.75
15d		2670 ± 220	3.72	-1.14

^aUnless stated otherwise, all results of means are $n \geq 2$. ^ccLogP values were calculated using ChemDraw 18.1. ^dLipophilic ligand efficiency = $-\log(\text{IC}_{50}) - \text{cLogP}$. Control compound used: **I-BET726** (IC₅₀: 0.01 μM).

As described above, we also had the single enantiomers of compounds **5** and **15c**. There was a modest level of chiral recognition shown with the (*R*)-enantiomer being the eutomer in both cases (Table 3). (*R*)-**15c** proved to be the highest affinity compound of this study with an IC₅₀

of 14.1 μM , making it 190-fold more potent than NMP itself (dose response curves of **15c**, (*R*)-**15c** and (*S*)-**15c** are available in Supplementary Figure S3).

Table 3. Assay data on resolved isomers.



Compound Number	R=	IC ₅₀ (μM \pm SEM) ^a	cLogP ^c	LLE ^d
5		1140 \pm 6	1.16	1.78
(<i>R</i>)- 5		629 \pm 26 ^b	1.16	2.04
(<i>S</i>)- 5		1430 \pm 170	1.16	1.69
15c		51.6 \pm 2.5	2.35	1.75
(<i>R</i>)- 15c		14.1 \pm 0.3	2.35	2.50
(<i>S</i>)- 15c		35.2 \pm 1.3	2.35	2.10

^aUnless stated otherwise, all results of means are $n \geq 2$. ^bSD reported. ^ccLogP values were calculated using ChemDraw 18.1. ^dLipophilic ligand efficiency = $-\log(\text{IC}_{50}) - \text{cLogP}$. Control compound used: **I-BET726** (IC₅₀: 0.01 μM).

With the elaboration of the phenyl NMP structure, we were interested to see how the structural modifications impacted the efficiency metrics. While **5** has an initial LLE of 1.78,

the increases in affinity, while associated with a growing molecular weight, also results in a rise in LLE due to the inclusion of the sulfonamide group (reducing cLogP), as shown in Table 1. Further substitution via Suzuki reactions gave further improved affinity, but at the expense of LLE (Table 2). Overall, the development of (*R*)-**15c** led to an improvement in affinity by over 2 orders of magnitude with an LLE of 2.50. From the perspective of fragment based elaboration this compares well to the development of BRD4 inhibitor **I-BET726** ($IC_{50} = 0.003 \mu\text{M}$, LLE = 1.93)[42] if considered as deriving from a racemic tetrahydroquinoline fragment ($IC_{50} = 158 \mu\text{M}$, LLE = 1.51).[43, 44]

2.3. X-ray Crystallography

We were able to gather a number of X-ray structures of our compound series to support the SAR studies of these compounds.

Firstly, a crystal structure of **5** bound to BRD4 BD1 was solved (Figure 2, Supplementary Video S2). The NMP segment of **5** retains the K-ac mimetic function, replicating the interactions between Asn140 and Tyr97. The phenyl group moiety of **5** emerges from the pocket and rests on the WPF shelf and appears to form weak interactions of its own with the WPF shelf residues Trp81 and Pro82 and the gatekeeper residue Ile146. While **5** was submitted as a racemic mixture, only the (*R*)-enantiomer was observed in the X-ray crystal structure of BRD4 BD1. This observation is consistent with the binding activity acquired from both (*R*)-**5** and (*S*)-**5**. The (*S*)-isomer in this pose would have more than likely produced a steric clash with the wall created by the ZA loop.

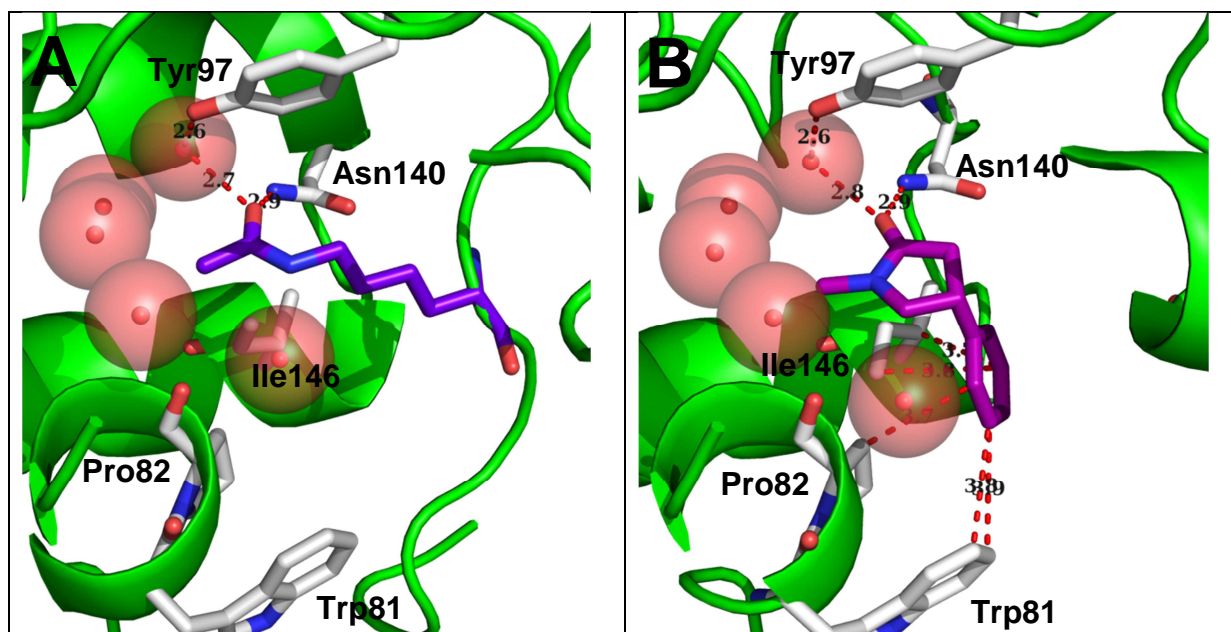
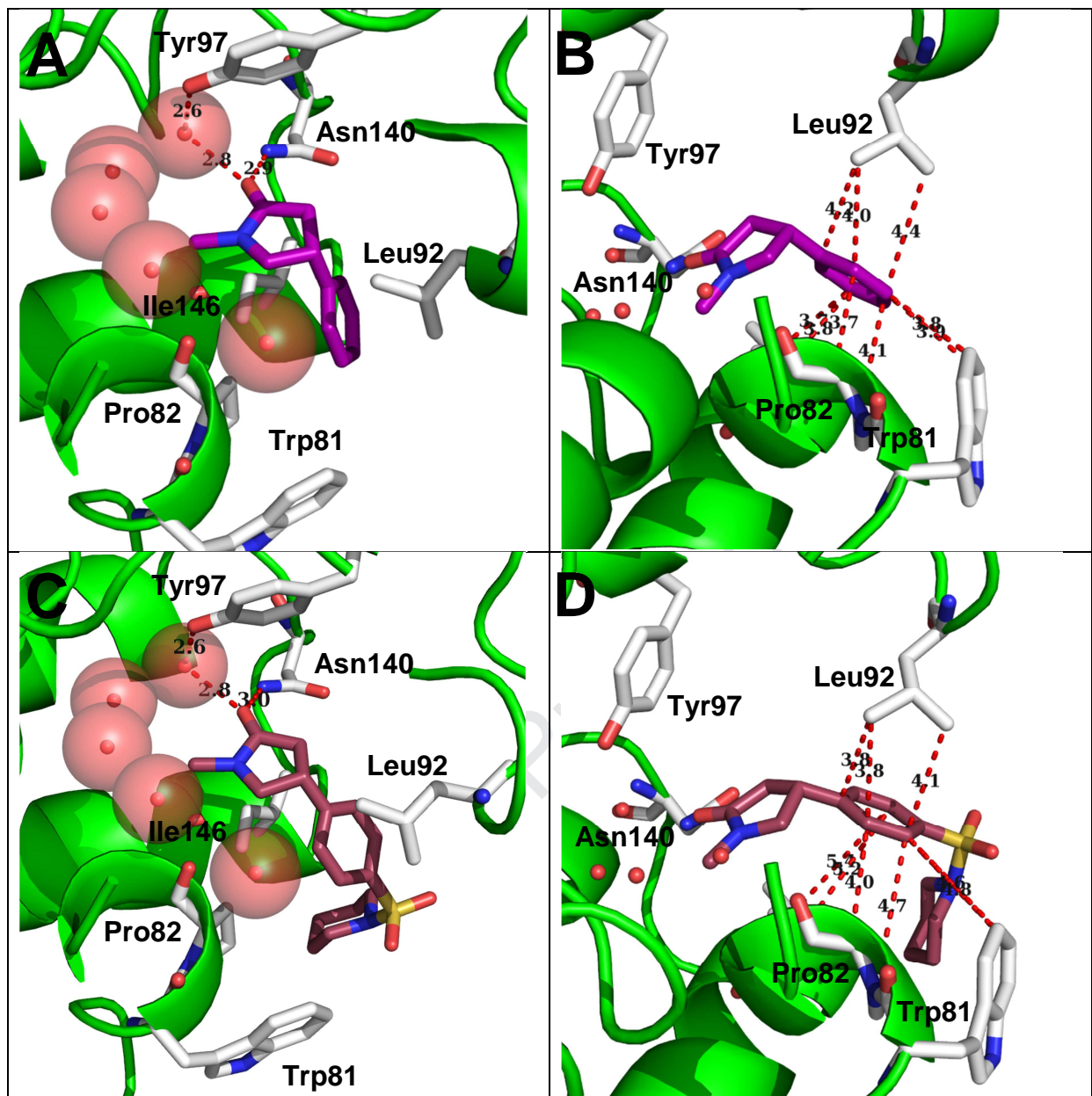


Figure 2. Comparison of binding substrates in BRD4 BD1. [A] K-ac (purple blue) (PDB: 3UVW). [B] (*R*)-**5** (purple, resolution: 1.5 Å). Water molecules shown as red spheres. Pro86, Val87 and Asp88 were hidden for better visualisation. Distances in Å, highlighted by red dashes.

Crystal structures of the sulfonamides **7b** and **7h** were also solved. As shown in Figure 3, only the (*R*)-isomer was evident in these co-crystal structures and the orientation of the NMP ring in the binding pocket matches closely with compound **5**. Despite the NMP backbone atoms overlaying closely (RMS = 0.20 and 0.37, respectively), the phenyl group appears to have shifted slightly (RMS = 1.25 and 1.63, respectively). This change has positioned the phenyl group closer towards the side chain of Leu92, but further away from Trp81, Pro82 and Ile146. Both the piperidyl group of **7b** and *n*-propyl moiety of **7h** rest in a pocket adjacent to the WPF shelf and form weak vdW interactions with Trp81, Asp145 and Met149 (Figure 4, Supplementary Video S3).



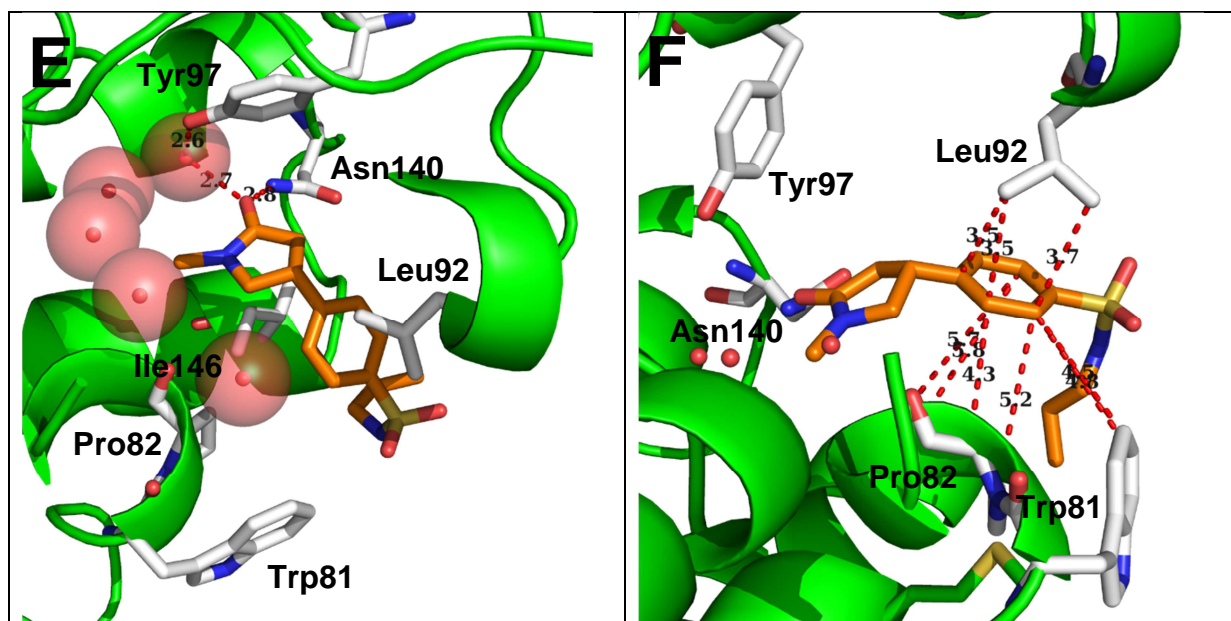


Figure 3. Comparison of X-ray crystal structures of NMP derivatives. [A, C, E] Binding site.

Pro86, Val87 and Asp88 were hidden for better visualisation. [B, D, F] Emphasis on phenyl group. [A, B] **5** (purple, resolution: 1.5 Å). [C, D] (*R*)-**7b** (raspberry, resolution: 1.55 Å). [E, F] (*R*)-**7h** (orange, resolution: 1.59 Å). Water molecules shown as red spheres. Distances in Å, highlighted by red dashes.

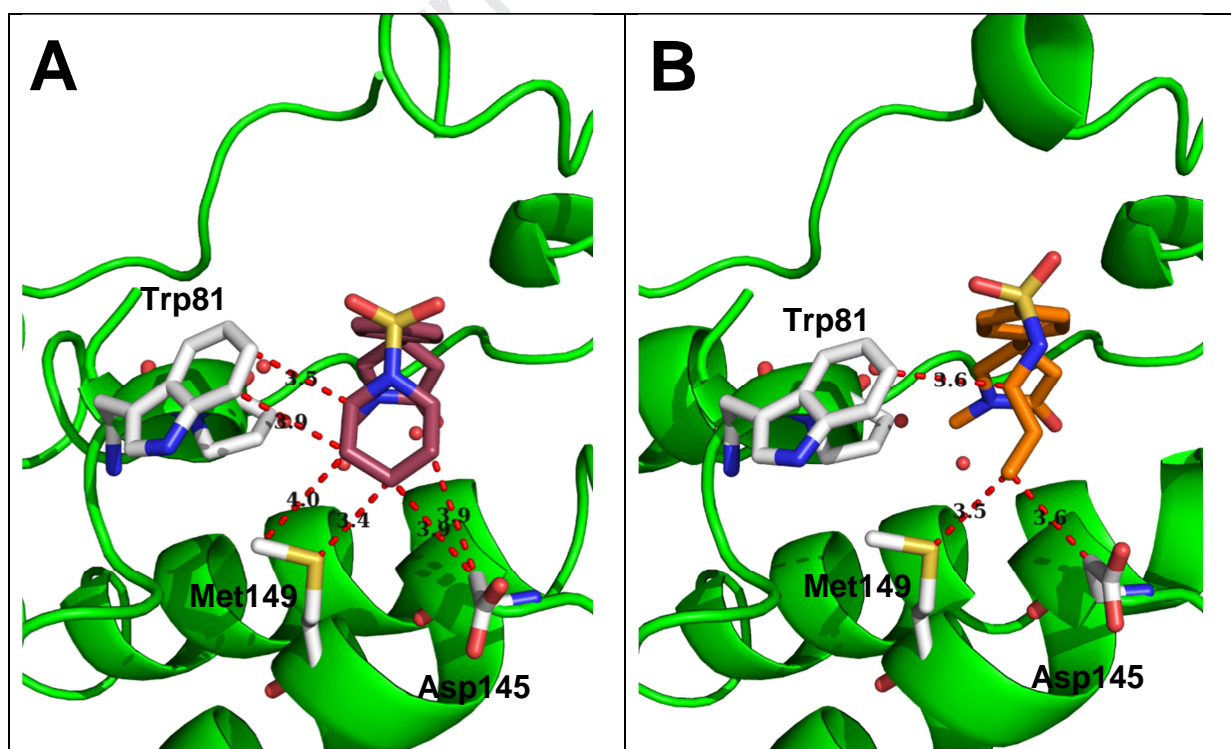


Figure 4. X-ray crystal structures illustrating the interactions between sulfonamide alkyl moieties and BRD4 BD1. [A] (*R*)-**7b** (raspberry, resolution: 1.55 Å). [B] (*R*)-**7h** (orange, resolution: 1.59 Å). Water molecules shown as red spheres. Distances in Å, highlighted by red dashes.

Finally, we were able to obtain a co-crystal structure of our highest affinity compound, **15c** (Figure 5 and Supplementary Video S4). To our surprise, the inclusion of the dimethoxyphenyl moiety had completely changed the orientation of the molecule. The dimethoxyphenyl group fills the acetamide binding pocket, using the two oxygen atoms to form a pair of hydrogen bonds to Asn140. The sulfonamide was re-oriented into the ZA channel, with the sulfonyl forming a hydrogen bond with the backbone nitrogen of Asp88 and the diethyl group lining up against Gln85. One of the ethyl moieties is situated in a small pocket that is in close proximity to three backbone carbonyls: Pro82, Gln85 and Pro86. Finally, the NMP segment rested in the pocket adjacent to Trp81, close to the sulfur atom of Met149. Again, submitted as a racemate, the (*S*)-enantiomer is observed in the co-crystal (Figure 6), although (*S*)-**15c** was found to have lower affinity than (*R*)-**15c** albeit only 2-fold. This is potentially due to the differences in crystallisation and assay conditions (electron density maps can be found in Supplementary Figure S4).

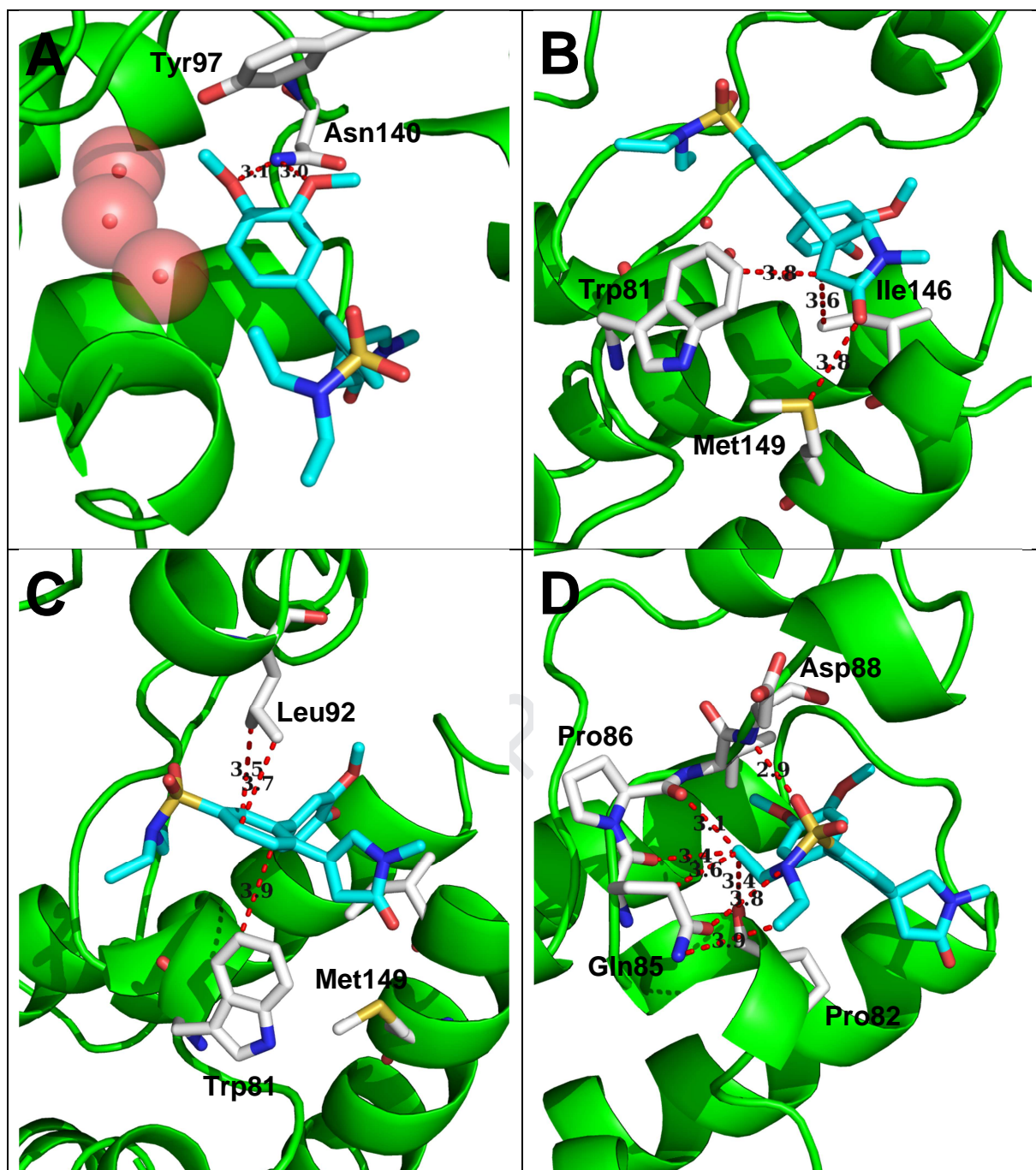


Figure 5. X-ray crystal structure of (*S*)-**15c** (cyan, resolution: 1.48 Å) bound to BRD4 BD1, illustrating interactions with the bromodomain. [A] Binding site. Pro86, Val87 and Asp88 were hidden for better visualisation. [B] NMP. [C] Phenyl ‘hub’. [D] Sulfonamide. Water molecules shown as red spheres. Distances in Å, highlighted by red dashes.

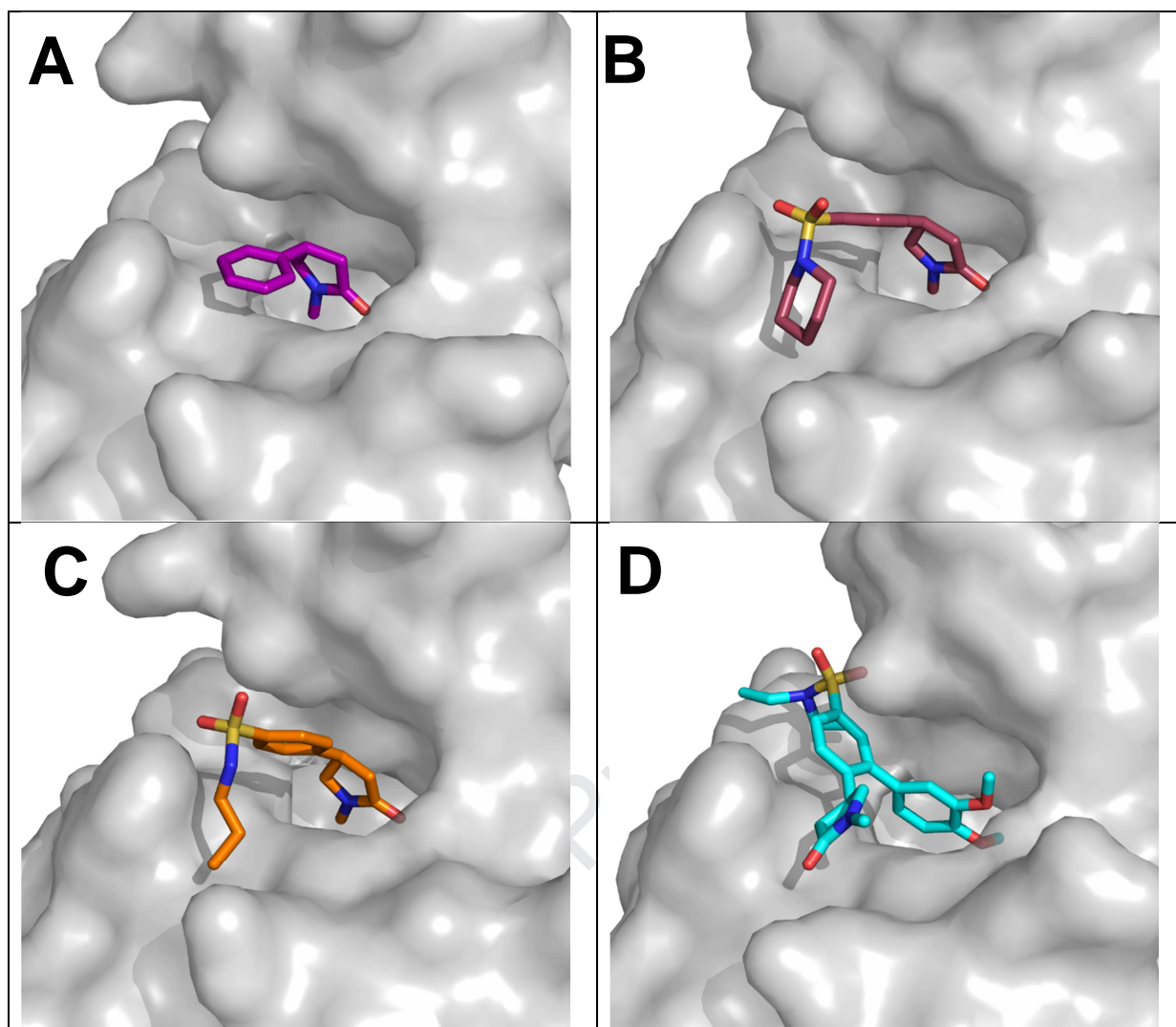
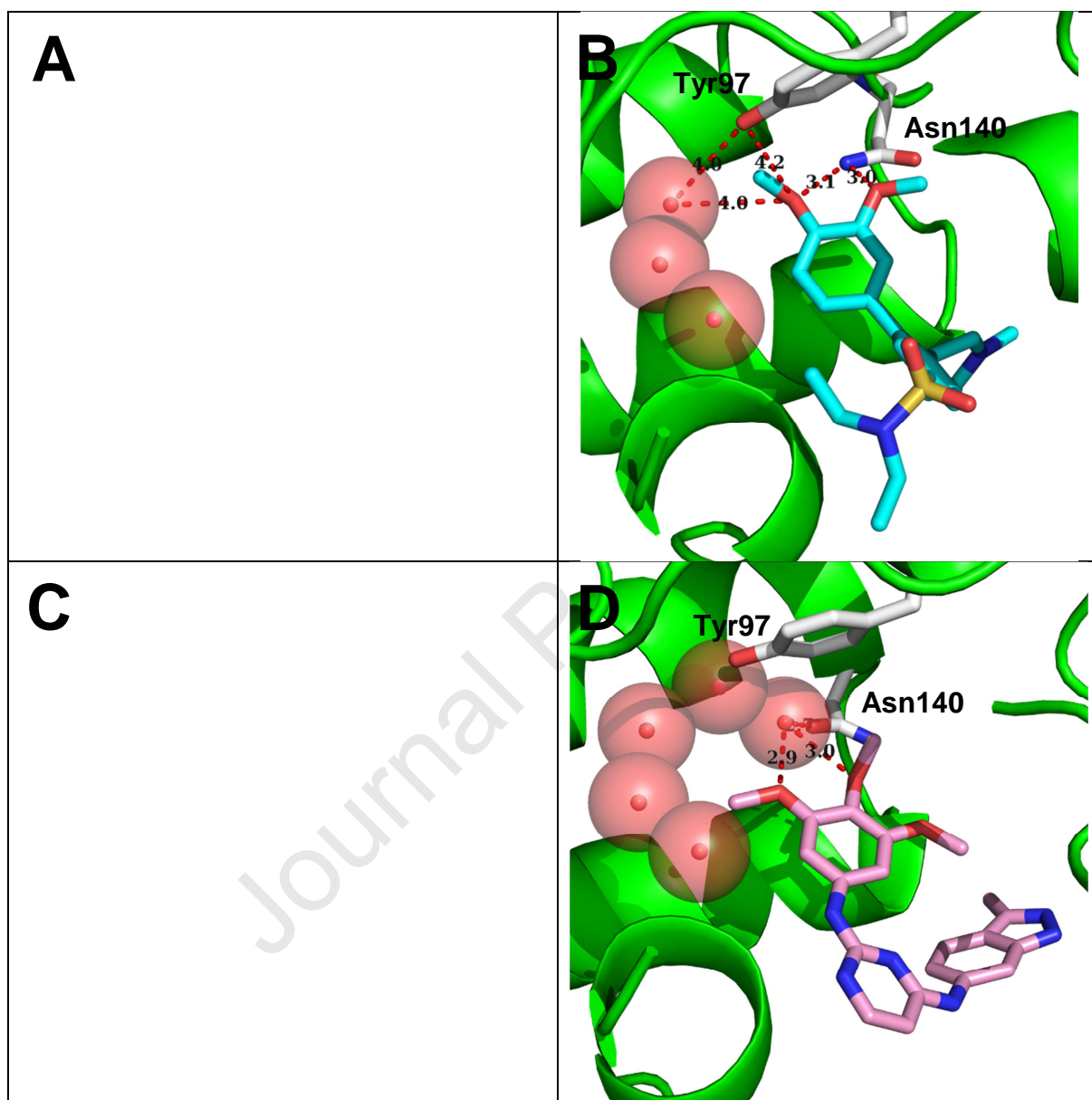


Figure 6. Comparison of X-ray crystal structures of bound NMP isomers in BRD4 BD1. [A] (*R*)-**5** (purple, resolution: 1.5 Å). [B] (*R*)-**7b** (raspberry, resolution: 1.55 Å). [C] (*R*)-**7h** (orange, resolution: 1.59 Å). [D] (*S*)-**15c** (cyan, resolution: 1.48 Å).

The presence of catechol ethers as acetamide mimics in BET inhibitors is preceded. The kinase inhibitor **GW612286X** was assessed among other inhibitors by Ember et al.[45] for BET inhibition. In their crystallographic studies, the trimethoxy group of **GW612286X** served as the K-ac mimetic in the binding pocket of BRD4 BD1. Chen et al.[46] evaluated the trimethoxy group as a mimetic for novel BRD4 inhibitors. In one of their compounds, **DC-BD-29**, the 3- and 4-methoxy groups also formed the dual interaction to Asn140 seen in **15c**. While the catechol ether of each compound fits in the binding pocket of BRD4 BD1,

they all have subtle differences with how they interact with the conserved tyrosine and asparagine residues (Figure 7).



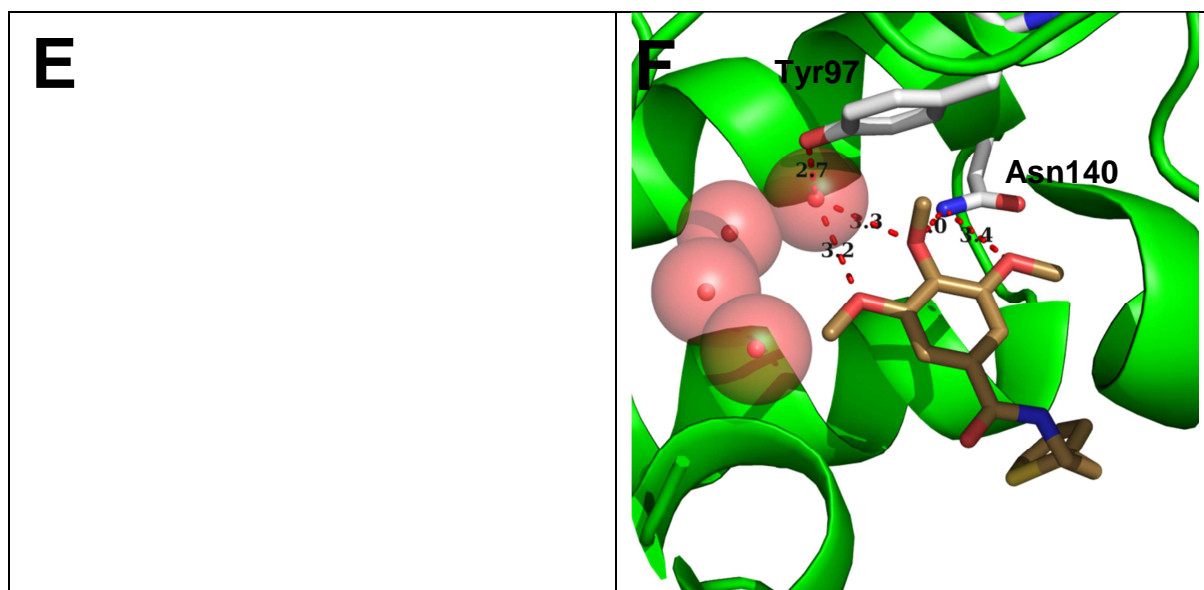


Figure 7. Comparison of catechol ether groups bound to BRD4 BD1. [A, B] (*S*)-**15c** (cyan, resolution: 1.48 Å). [C, D] **GW612286X** (pink) (PDB: 4O78). [E, F] **DC-BD-29** (sand) (PDB: 5H21). [A, C, E] Chemical structure. [B, D, F] Binding site. Water molecules shown as red spheres. Pro86, Val87 and Asp88 were hidden for better visualisation. Distances in Å, highlighted by red dashes.

3. Conclusion

BRD4 is a well-characterised target for FBDD approaches and provides a useful exemplar of bromodomain inhibitor discovery in general.[21, 47, 48] NMP itself has been co-crystallised with several bromodomains and could be a starting point for campaigns against each one. Here, we have tested these principles with a 4-phenyl derivative of NMP.

We devised a synthetic strategy built around electrophilic aromatic substitution as a chemically tractable way to introduce functionality into the “naked” ring of **5** which is available in multigram quantities. We were able to go from a mono-substituted precursor to a tri-substituted analogues series, and in doing so, improve affinity 190-fold with just 30 compounds prepared. In terms of efficiency metrics, it is notable that the increase affinity has come with a well preserved LLE with the sulfonamide, a positive influence in keeping the

logP of analogues down. As a proof-of-concept, this work supports further investigation of direct aromatic substitution reactions to drive FBDD programs forward. Here, we have utilised the *ortho*- and *para*- directing effects of the NMP group to create the vectors, but other means of ring activation could generate pathways to *meta* substitution, relative to the NMP group. The chiral nature of the precursor compound **5** might typically be considered a disincentive to progression in an FBDD campaign, but here, we show that ready access to both enantiomers gave rise to pairs of analogues that could be assessed either as racemates or, where warranted, in enantiopure form.

Crystallography was also an important support for the development of the series with the elaboration of NMP to **5** and subsequently to **7e** showing the expected poses in response to structure elaboration. In an unexpected turn, a crystal structure of the lead compound **15c** adopted a new binding orientation in the BRD4 bromodomain pocket. This change provides a clear explanation of the SAR surrounding the tri-substituted compounds **14** and **15** and shows that the tri-substituted aryl ring is perhaps not the best for preserving the NMP group in the acetamide pocket. On the other hand, **15c** itself may prove an excellent new starting point for analogue design projecting the sulfonamide and NMP “vectors” in potentially productive directions.

4. Experimental

4.1. Chemistry

^1H and ^{13}C Nuclear Magnetic Resonance spectra were conducted on a Bruker Advance III Nanobay 400 MHz spectrometer coupled to the BACS 60 automatic sample changer and obtained at 400.1 MHz and 100.6 MHz. All spectra were processed using MestReNova 6.0 software. The chemical shifts of all ^1H were measured relative to the expected solvent peaks of the respective NMR solvents; CDCl_3 , 7.26; MeOD, 3.31; DMSO, 2.50. The chemical shifts of all ^{13}C were measured relative to the expected solvent peaks of the respective NMR solvents; CDCl_3 , 77.2; MeOD, 49.0; DMSO, 39.5. The data for all spectra are reported in the following format: chemical shift (integration, multiplicity, coupling constant, assignment). Multiplicity is defined as; s = singlet, d = doublet, t = triplet, q = quartet, quint = quintet, dd = doublet of doublets, dt = doublet of triplets, td = triplet of doublets, tt = triplet of triplets, qd = quartet of doublets, ddd = doublet of doublet of doublets, m = multiplet. Coupling constants are applied as J in Hertz (Hz). For ^1H and ^{13}C spectra, refer to Supplementary Figure S5.

All HRMS analyses were done on an Agilent 6224 TOF LC/MS Mass Spectrometer coupled to an Agilent 1290 Infinity (Agilent, Palo Alto, CA). All data were acquired and reference mass corrected via a dual-spray electrospray ionisation (ESI) source. Each scan or data point on the Total Ion Chromatogram (TIC) is an average of 13,700 transients, producing a spectrum every second. Mass spectra were created by averaging the scans across each peak and background subtracted against the first 10 seconds of the TIC. Acquisition was performed using the Agilent Mass Hunter Data Acquisition software version B.05.00 Build 5.0.5042.2 and analysis was performed using Mass Hunter Qualitative Analysis version B.05.00 Build 5.0.519.13.

All LCMS analyses were carried out on an Agilent 6100 Series Single Quad LC/MS coupled with an Agilent 1200 Series HPLC, 1260 Infinity G1312B Binary pump, 1260 Infinity G1367E 1260 HiP ALS autosampler and 1290 Infinity G4212A 1290 DAD detector. The liquid chromatography conditions were: reverse phase HPLC analysis fitted with a Luna C8(2) 5 μ L 50 X 4.6 mm 100Å at a temperature of 30 °C. The sample injection volume was 5 μ L, which was run in 0.1% formic acid in acetonitrile at a gradient of 5-100% over 10 minutes. Detection methods were either 254 nm or 214 nm. The mass spectrum conditions were: Quadrupole ion source with Multimode-ES. The drying gas temperature was 300 °C and the vaporizer temperature was 200 °C. The capillary voltage in positive mode was 2000V, while in negative mode, the capillary voltage was 4000V. The scan range was 100-1000 m/z with a step size of 0.1 second over 10 minutes.

TLCs were carried on Merck TLC Silica gel 60 F₂₅₄ plates using the appropriate mobile phase. Purification by column chromatography was conducted with Davisil Chromatographic Silica LC60A (40-63 micron) using the specified mobile phases.

Purification on reverse-phase HPLC was done on a Waters Delta Prep 2000 Prep HPLC System that was fitted with a Waters Delta Prep 2000 Pump and Controller. Samples were injected into a Waters Prep Rack with Manual Injector, which were run through a Luna C8(2) 10 μ L 50 X 21.20 mm 100Å and Waters 486 Tunable Absorbance Detector. The conditions were: Solvent A (0.1% TFA in H₂O) and Solvent B (0.1% TFA in CH₃CN), with a gradient of 0-80% Solvent B over a 20-minute period.

Compound purity was determined using an Agilent 1260 Infinity Analytical HPLC (1260 Infinity G1322A Degasser, 1260 Infinity G1312B Binary pump, G1367E HiP ALS autosampler, 1260 Infinity G1316A Thermostatted Column Compartment, and 1260 Infinity G4212B DAD detector. The liquid chromatography conditions were: reverse phase HPLC

analysis fitted with a Zorbax Eclipse Plus C18 Rapid Resolution 4.6 X 100 mm 3.5-Micron. The sample injection volume was 1 μ L, which was run in Solvent A (0.1% TFA in H₂O) and Solvent B (0.1% TFA in CH₃CN), with a gradient of 5-100% Solvent B over a 10-minute period. All compounds submitted for assays and X-ray crystallography studies were assessed for purity of 95% or greater on 214 nm and 254 nm.

Separation on chiral HPLC was done on an Agilent 1260 Infinity Prep HPLC (1260 Infinity G1361A Prep Pump, 1260 Infinity G2260A Prep ALS, 1260 Infinity G1328C Man Inj, 1260 Infinity G1315D DAD VL, and 1260 Infinity G1364B FC-PS). The liquid chromatography conditions were: normal phase HPLC analysis fitted with a Phenomenex Lux 5 μ m Cellulose-1 4.6 x 150 mm. The sample injection volume was 10 μ L at a concentration of 1 mg/mL, which was run in Solvent A (40% petroleum ether) and Solvent B (60% ethanol), over a 10-minute period.

Specific rotations were measured using a Jasco P-2000 polarimeter. The light source was a sodium lamp with a wavelength of 589 nm. Compounds were loaded into a 3.5 mm x 100 mm cylindrical glass cell. Digital integration time was 5 seconds per cycle for 10 cycles.

4.1.1. Methyl 4-nitro-3-phenylbutanoate (**2**)

Methyl *trans*-cinnamate **1** (5.01 g, 30.9 mmol) was weighed into a 250 mL round-bottom flask with a magnetic stir-bar and dissolved in nitromethane (17 mL, 0.308 mol), to which stirring commenced. 1,1,3,3-tetramethylguanidine (775 μ L, 6.18 mmol) was added, and the mixture was left to stir for 42 hours at room temperature, checking for completion with TLC. After completion, the mixture was quenched with 5% HCl (75 mL) and washed with diethyl ether (3 x 75 mL). The organic layers were combined, dried with MgSO₄, filtered and concentrated under reduced pressure to afford an orange-coloured oil. The oil was then purified using column chromatography (Mobile phase: 10% EtOAc in petroleum benzene,

TLCs were checked in 20% EtOAc in petroleum benzene) to afford **2** (5.62 g, 82%) as a clear oil. $^1\text{H NMR}$ (400 MHz, CDCl_3) δ 7.37 – 7.21 (m, 5H), 4.70 (ddd, $J = 20.5, 12.6, 7.5$ Hz, 2H), 3.99 (quint, $J = 7.4$ Hz, 1H), 3.64 (s, 3H), 2.83 – 2.74 (m, 2H) ppm. $^{13}\text{C NMR}$ (101 MHz, CDCl_3) δ 171.2, 138.4, 129.2, 128.2, 127.4, 79.5, 52.1, 40.3, 37.6 ppm.

4.1.2. 4-phenylpyrrolidin-2-one (**4**)

A two-neck 250 mL round-bottom flask with a stir-bar was purged with N_2 , to which palladium on carbon (10%, 453 mg) was added and submerged in a minimum amount of dichloromethane. Methyl 4-nitro-3-phenylbutanoate **2** (4.53 g, 20.3 mmol) was dissolved in acetic acid (150 mL) and pipetted into the flask while keeping it under N_2 . The flask was purged three more times with N_2 and then purged with H_2 three times, to which the contents were left to stir at room temperature. The progress of the reaction was monitored by NMR. After completion, the flask was purged with N_2 three times and the contents filtered carefully through a glass microfiber filter paper under very gentle vacuum. The filtered palladium catalyst was washed with dichloromethane then separately quenched with H_2O while the filtrate was concentrated under reduced pressure to give methyl 4-amino-3-phenylbutanoate (**3**) as a caramel-coloured oil. In a 250 mL round-bottom flask, the oil was then taken up in EtOH (75 mL) and Et_3N (1 mL) and then heated under reflux overnight. Upon assessing completion via LCMS, the mixture was concentrated under reduced pressure, then purified with a silica column (Mobile phase: neat EtOAc) to afford the lactam **4** (2.73 g, 83%) as an orange crystalline solid. $^1\text{H NMR}$ (400 MHz, CDCl_3) δ 7.54 (br s, 1H), 7.36 – 7.29 (m, 2H), 7.28 – 7.21 (m, 3H), 3.82 – 3.74 (m, 1H), 3.66 (dt, $J = 16.9, 8.6$ Hz, 1H), 3.41 (dd, $J = 9.5, 7.3$ Hz, 1H), 2.73 (dd, $J = 16.9, 8.9$ Hz, 1H), 2.50 (dd, $J = 16.9, 8.8$ Hz, 1H) ppm. $^{13}\text{C NMR}$ (101 MHz, CDCl_3) δ 178.3, 142.2, 128.8, 127.0, 126.8, 49.7, 40.2, 38.2 ppm. **ESI-MS**: m/z 162.1 $[\text{M}+\text{H}]^+$.

4.1.3. Lactam Methylation

In a round-bottom flask with a magnetic stir-bar, 4-phenylpyrrolidin-2-one **4** was weighed out and dissolved in THF. The flask was partially sealed with a rubber septum, purged with N₂ and placed on an ice-bath. Sodium hydride (2 mol. eq., 60% dispersed in mineral oil) was added to the mixture under N₂ and the contents were stirred for 30 minutes. Iodomethane (5 mol. eq.) was then added via syringe, and the contents were stirred at room temperature overnight. After completion, the THF was removed under reduced pressure. The resulting residue was quenched with 50% saturated aqueous NaCl and washed with EtOAc three times. The combined organic layers were dried with MgSO₄, filtered and concentrated under reduced pressure to obtain the crude product, which was then purified with silica column chromatography (Mobile phase: 20% petroleum benzene in EtOAc) to afford the respective products.

4.1.3.1. 1-methyl-4-phenylpyrrolidin-2-one (**5**)

Acquired 1.44 g (88%) as a clear oil from 1.51 g of **4**. **¹H NMR** (400 MHz, CDCl₃) δ 7.37 – 7.31 (m, 2H), 7.29 – 7.20 (m, 3H), 3.75 (dd, *J* = 9.6, 8.3 Hz, 1H), 3.58 (dt, *J* = 16.9, 8.4 Hz, 1H), 3.41 (dd, *J* = 9.6, 7.0 Hz, 1H), 2.91 (s, 3H), 2.82 (dd, *J* = 16.9, 9.1 Hz, 1H), 2.55 (dd, *J* = 16.9, 8.3 Hz, 1H) ppm. **¹³C NMR** (101 MHz, CDCl₃) δ 174.1, 142.6, 129.0, 127.21, 126.85, 56.9, 38.9, 37.3, 29.7 ppm. **ESI-MS**: *m/z* 176.2 [M+H]⁺; **HR-MS**: *m/z* calcd. for C₁₁H₁₃NO [M+H]⁺: 175.0997; found 175.0992. **HPLC** (PP gradient, MeOH): 4.87 min.

4.1.3.2. (*R*)-1-methyl-4-phenylpyrrolidin-2-one ((*R*)-**5**)

Acquired 40.9 mg (85%) as a clear oil from 44.3 mg of (*R*)-**4**. [α]_D²⁵ - 38.4 (*c* 1, CHCl₃). **¹H NMR** (400 MHz, CDCl₃) δ 7.37 – 7.30 (m, 2H), 7.29 – 7.20 (m, 3H), 3.74 (dd, *J* = 9.6, 8.3 Hz, 1H), 3.57 (dt, *J* = 16.9, 8.4 Hz, 1H), 3.40 (dd, *J* = 9.6, 7.0 Hz, 1H), 2.90 (s, 3H), 2.81 (dd, *J* = 16.9, 9.1 Hz, 1H), 2.54 (dd, *J* = 16.8, 8.3 Hz, 1H) ppm. **¹³C NMR** (101 MHz, CDCl₃) δ

174.0, 142.7, 129.0, 127.18, 126.83, 56.8, 38.9, 37.3, 29.7 ppm. **ESI-MS**: m/z 176.0 $[M+H]^+$; **HR-MS**: m/z calcd. for $C_{11}H_{13}NO$ $[M+H]^+$: 175.0997; found 175.0996. **HPLC** (PP gradient, MeOH): 4.67 min.

4.1.3.3. (*S*)-1-methyl-4-phenylpyrrolidin-2-one ((*S*)-**5**)

Acquired 23.5 mg (85%) as a clear oil from 25.3 mg of (*S*)-**4**. $[\alpha]_D^{24} + 43.2$ (c 0.5, $CHCl_3$). **1H NMR** (400 MHz, $CDCl_3$) δ 7.37 – 7.29 (m, 2H), 7.29 – 7.19 (m, 3H), 3.74 (dd, $J = 9.6, 8.3$ Hz, 1H), 3.57 (dt, $J = 16.9, 8.4$ Hz, 1H), 3.40 (dd, $J = 9.6, 7.0$ Hz, 1H), 2.90 (s, 3H), 2.81 (dd, $J = 16.9, 9.1$ Hz, 1H), 2.54 (dd, $J = 16.8, 8.3$ Hz, 1H) ppm. **^{13}C NMR** (101 MHz, $CDCl_3$) δ 174.0, 142.7, 129.0, 127.17, 126.82, 56.8, 38.9, 37.3, 29.7 ppm. **ESI-MS**: m/z 176.0 $[M+H]^+$; **HR-MS**: m/z calcd. for $C_{11}H_{13}NO$ $[M+H]^+$: 175.0997; found 175.0994. **HPLC** (PP gradient, MeOH): 4.71 min.

4.1.4. Sulfonamide Formation

1-methyl-4-phenylpyrrolidin-2-one **5** was weighed in a 25 mL round-bottom flask and dissolved in CH_2Cl_2 (5 mL). Chlorosulfonic acid (8 mol. eq.) was then slowly pipetted into the mixture at room temperature and left to stir overnight. After this time, the mixture was slowly quenched with water (25 mL) at 0 °C and washed with CH_2Cl_2 (3 x 25 mL). The combined organic layers were dried with $MgSO_4$, filtered and concentrated under reduced pressure to acquire the sulfonyl chloride **6** as an oil. This was then re-taken up in CH_2Cl_2 (15mL) and the appropriate amine (10 mol. eq.) was added, followed by Et_3N (5 mol. eq.). The mixture was left to stir overnight, quenched in water (20 mL)^a and then washed with CH_2Cl_2 (3 x 20 mL). The organic layers were combined, dried with $MgSO_4$, filtered and concentrated under reduced pressure to afford each sulfonamide as an oil or a solid. These were purified using the specified methods to afford the sulfonamides **7a-7n**.

4.1.4.1. *N,N*-diethyl-4-(1-methyl-5-oxopyrrolidin-3-yl)benzenesulfonamide (**7a**)

Acquired 42.8 mg (30%) as a brown oil from 80.0 mg of **5** using diethylamine as the amine (Mobile phase: 1% MeOH in CH₂Cl₂). **¹H NMR** (400 MHz, CDCl₃) δ 7.75 (d, *J* = 8.4 Hz, 2H), 7.33 (d, *J* = 8.2 Hz, 2H), 3.77 (dd, *J* = 9.7, 8.3 Hz, 1H), 3.67 – 3.57 (m, 1H), 3.39 (dd, *J* = 9.8, 6.5 Hz, 1H), 3.21 (q, *J* = 7.2 Hz, 4H), 2.90 (s, 3H), 2.83 (dd, *J* = 16.9, 9.2 Hz, 1H), 2.50 (dd, *J* = 16.9, 7.7 Hz, 1H), 1.11 (t, *J* = 7.1 Hz, 6H) ppm. **¹³C NMR** (101 MHz, CDCl₃) δ 173.3, 147.4, 139.3, 127.74, 127.48, 56.3, 42.2, 38.6, 37.0, 29.7, 14.3 ppm. **ESI-MS**: *m/z* 311.0 [M+H]⁺. **HR-MS**: *m/z* calc. for C₁₅H₂₂N₂O₃S [M+H]⁺: 310.1351; found 310.1359. **HPLC** (PP gradient, MeOH): 5.44 min.

4.1.4.1.1. *Upscaled Formation of 7a*

1-methyl-4-phenylpyrrolidin-2-one **5** (578 mg, 3.30 mmol) was weighed in a 100 mL round-bottom flask and dissolved in CH₂Cl₂ (20 mL). Chlorosulfonic acid (3.07 g, 1.76 mL, 8 mol. eq.) was then slowly pipetted into the mixture at room temperature and left to stir overnight. After this time, the mixture was slowly quenched with water (50 mL) at 0 °C and washed with CH₂Cl₂ (3 x 50 mL). The combined organic layers were dried with MgSO₄, filtered and concentrated under reduced pressure to acquire the sulfonyl chloride **6** as an oil. This was then re-taken up in CH₂Cl₂ (40 mL) and diethylamine (2.41 g, 3.41 mL, 10 mol. eq.) was added, followed by Et₃N (1.67 g, 2.30 mL, 5 mol. eq.). The mixture was left to stir overnight, then quenched in water (50 mL) and washed with CH₂Cl₂ (3 x 50 mL). The organic layers were combined, dried with MgSO₄, filtered and concentrated under reduced pressure to afford the crude product as an oil. This were purified using the same conditions as previously described to afford **7a** (630 mg, 62%) as a clear oil.

4.1.4.2. *1*-methyl-4-(4-(piperidin-1-ylsulfonyl)phenyl)pyrrolidin-2-one (**7b**)

Acquired 94.6 mg (64%) as a yellow solid from 80.5 mg of **5** using piperidine as the amine (Mobile phase: EtOAc). **¹H NMR** (400 MHz, CDCl₃) δ 7.68 (d, *J* = 8.4 Hz, 2H), 7.35 (d, *J* = 8.2 Hz, 2H), 3.77 (dd, *J* = 9.7, 8.3 Hz, 1H), 3.63 (dt, *J* = 16.0, 8.2 Hz, 1H), 3.39 (dd, *J* = 9.8, 6.5 Hz, 1H), 2.98 – 2.91 (m, 4H), 2.88 (s, 3H), 2.82 (dd, *J* = 16.9, 9.2 Hz, 1H), 2.49 (dd, *J* = 16.8, 7.8 Hz, 1H), 1.66 – 1.55 (m, 4H), 1.44 – 1.34 (m, 2H) ppm. **¹³C NMR** (101 MHz, CDCl₃) δ 173.2, 147.7, 135.2, 128.33, 127.40, 56.1, 46.9, 38.6, 37.0, 29.7, 25.2, 23.5 ppm. **ESI-MS**: *m/z* 323.0 [M+H]⁺. **HR-MS**: *m/z* calc. for C₁₆H₂₂N₂O₃S [M+H]⁺: 322.1351; found 322.1356. **HPLC** (PP gradient, MeOH): 5.63 min.

4.1.4.3. *1-methyl-4-(4-(morpholin sulfonyl)phenyl)pyrrolidin-2-one (7c)*

Acquired 69.9 mg (52%) as a yellow solid from 72.3 mg of **5** using morpholine as the amine (Mobile phase: 2% MeOH in CH₂Cl₂). **¹H NMR** (400 MHz, CDCl₃) δ 7.68 (d, *J* = 8.4 Hz, 2H), 7.38 (d, *J* = 8.2 Hz, 2H), 3.77 (dd, *J* = 9.7, 8.3 Hz, 1H), 3.74 – 3.57 (m, 5H), 3.38 (dd, *J* = 9.8, 6.5 Hz, 1H), 3.01 – 2.91 (m, 4H), 2.88 (s, 3H), 2.83 (dd, *J* = 16.9, 9.2 Hz, 1H), 2.49 (dd, *J* = 16.8, 7.6 Hz, 1H) ppm. **¹³C NMR** (101 MHz, CDCl₃) δ 173.2, 148.3, 133.9, 128.56, 127.61, 66.1, 56.1, 46.0, 38.5, 37.0, 29.7 ppm. **ESI-MS**: *m/z* 324.9 [M+H]⁺. **HR-MS**: *m/z* calc. for C₁₅H₂₀N₂O₄S [M+H]⁺: 324.1144; found 324.1154. **HPLC** (PP gradient, MeOH): 4.62 min.

4.1.4.4. *1-methyl-4-(4-((4-phenylpiperidin-1-yl)sulfonyl)phenyl)pyrrolidin-2-one (7d)*

Acquired 73.8 mg (63%) as a white solid from 51.0 mg of **5** using 4-phenylpiperidine as the amine (Mobile phase: EtOAc). **¹H NMR** (400 MHz, CDCl₃) δ 7.76 (d, *J* = 8.4 Hz, 2H), 7.40 (d, *J* = 8.2 Hz, 2H), 7.33 – 7.25 (m, 2H), 7.23 – 7.17 (m, 1H), 7.17 – 7.11 (m, 2H), 3.93 (d, *J* = 11.6 Hz, 2H), 3.81 (dd, *J* = 9.7, 8.3 Hz, 1H), 3.73 – 3.60 (m, 1H), 3.43 (dd, *J* = 9.7, 6.5 Hz, 1H), 2.93 (s, 3H), 2.87 (dd, *J* = 16.9, 9.2 Hz, 1H), 2.54 (dd, *J* = 16.9, 7.7 Hz, 1H), 2.49 – 2.32 (m, 3H), 1.93 – 1.76 (m, 4H) ppm. **¹³C NMR** (101 MHz, CDCl₃) δ 173.2, 147.8, 144.8,

135.2, 128.63, 128.42, 127.46, 126.67, 56.1, 46.9, 41.8, 38.6, 37.0, 32.5 (d, $J = 2.1$ Hz), 29.7 ppm. **ESI-MS**: m/z 398.9 $[M+H]^+$. **HR-MS**: m/z calc. for $C_{22}H_{26}N_2O_3S$ $[M+H]^+$: 398.1670; found 398.1664. **HPLC** (PP gradient, 1:1 $CH_3CN:H_2O$ with 0.1% formic acid): 6.75 min.

4.1.4.5. *4-(4-((3,4-dihydroquinolin-1(2H)-yl)sulfonyl)phenyl)-1-methylpyrrolidin-2-one (7e)*

Acquired 51.1 mg (48%) as a yellow gum from 50.1 mg of **5** using 1,2,3,4-tetrahydroquinoline as the amine (Mobile phase: EtOAc). **1H NMR** (400 MHz, $CDCl_3$) δ 7.77 (dd, $J = 8.3, 0.8$ Hz, 1H), 7.57 (d, $J = 8.5$ Hz, 2H), 7.26 – 7.22 (m, 2H), 7.22 – 7.16 (m, 1H), 7.08 (td, $J = 7.4, 1.2$ Hz, 1H), 7.04 – 6.99 (m, 1H), 3.83 – 3.79 (m, 2H), 3.76 (dd, $J = 9.8, 8.3$ Hz, 1H), 3.64 – 3.55 (m, 1H), 3.39 – 3.32 (m, 1H), 2.90 (s, 3H), 2.83 (dd, $J = 16.9, 9.3$ Hz, 1H), 2.52 – 2.42 (m, 3H), 1.68 – 1.64 (m, 2H) ppm. **^{13}C NMR** (101 MHz, $CDCl_3$) δ 173.3, 148.0, 138.7, 136.8, 130.7, 129.3, 127.81, 127.41, 126.66, 125.16, 124.79, 56.2, 46.7, 38.6, 36.9, 29.7, 26.7, 21.8 ppm. **ESI-MS**: m/z 370.8 $[M+H]^+$. **HR-MS**: m/z calc. for $C_{15}H_{22}N_2O_3S$ $[M+H]^+$: 370.1351; found 370.1357. **HPLC** (PP gradient, MeOH): 6.26 min.

4.1.4.6. *N-benzyl-4-(1-methyl-5-oxopyrrolidin-3-yl)benzenesulfonamide (7f)*

Acquired 68.9 mg (69%) as a white solid from 51.0 mg of **5** using benzylamine as the amine (Mobile phase: 2% MeOH in CH_2Cl_2). **1H NMR** (400 MHz, $CDCl_3$) δ 7.80 (d, $J = 8.4$ Hz, 2H), 7.31 (d, $J = 8.3$ Hz, 2H), 7.27 – 7.12 (m, 5H), 5.38 (br t, $J = 5.5$ Hz, 1H), 4.12 (d, $J = 5.4$ Hz, 2H), 3.77 (dd, $J = 9.7, 8.3$ Hz, 1H), 3.61 (dt, $J = 15.9, 8.1$ Hz, 1H), 3.38 (dd, $J = 9.8, 6.5$ Hz, 1H), 2.95 – 2.78 (m, 4H), 2.48 (dd, $J = 16.9, 7.7$ Hz, 1H) ppm. **^{13}C NMR** (101 MHz, $CDCl_3$) δ 173.5, 147.8, 139.0, 136.4, 128.71, 127.97, 127.93, 127.87, 127.56, 56.2, 47.3, 38.6, 37.0, 29.8 ppm. **ESI-MS**: m/z 344.9 $[M+H]^+$. **HR-MS**: m/z calc. for $C_{18}H_{20}N_2O_3S$ $[M+H]^+$: 344.1195; found 344.1198. **HPLC** (PP gradient, MeOH): 5.22 min.

4.1.4.7. *N-ethyl-4-(1-methyl-5-oxopyrrolidin-3-yl)benzenesulfonamide (7g)*

Acquired 46.4 mg (58%) as a white solid from 50.3 mg of **5** using ethylamine as the amine (Mobile phase: 2% MeOH in CH₂Cl₂). **¹H NMR** (400 MHz, CDCl₃) δ 7.82 (d, *J* = 8.4 Hz, 2H), 7.35 (d, *J* = 8.3 Hz, 2H), 5.01 (t, *J* = 6.0 Hz, 1H), 3.78 (dd, *J* = 9.7, 8.3 Hz, 1H), 3.64 (dt, *J* = 16.1, 8.2 Hz, 1H), 3.40 (dd, *J* = 9.8, 6.5 Hz, 1H), 2.98 (qd, *J* = 7.2, 6.1 Hz, 2H), 2.91 (s, 3H), 2.85 (dd, *J* = 17.0, 8.7 Hz, 1H), 2.52 (dd, *J* = 16.8, 7.7 Hz, 1H), 1.09 (t, *J* = 7.2 Hz, 3H) ppm. **¹³C NMR** (101 MHz, CDCl₃) δ 173.4, 147.7, 138.9, 127.74, 127.50, 56.2, 38.6, 38.2, 36.9, 29.7, 15.1 ppm. **ESI-MS**: *m/z* 282.9 [M+H]⁺. **HR-MS**: *m/z* calc. for C₁₃H₁₈N₂O₃S [M+H]⁺: 282.1038; found 282.1042. **HPLC** (PP gradient, MeOH): 4.17 min.

4.1.4.8. 4-(1-methyl-5-oxopyrrolidin-3-yl)-*N*-propylbenzenesulfonamide (**7h**)

Acquired 40.5 mg (59%) as a white solid from 40.3 mg of **5** using *n*-propylamine as the amine (Mobile phase: 2% MeOH in CH₂Cl₂). **¹H NMR** (400 MHz, CDCl₃) δ 7.83 (d, *J* = 8.5 Hz, 2H), 7.36 (d, *J* = 8.2 Hz, 2H), 4.82 (t, *J* = 6.1 Hz, 1H), 3.79 (dd, *J* = 9.8, 8.3 Hz, 1H), 3.65 (dt, *J* = 16.1, 8.2 Hz, 1H), 3.41 (dd, *J* = 9.8, 6.5 Hz, 1H), 2.95 – 2.82 (m, 6H), 2.52 (dd, *J* = 16.9, 7.7 Hz, 1H), 1.55 – 1.43 (m, 2H), 0.86 (t, *J* = 7.4 Hz, 3H) ppm. **¹³C NMR** (101 MHz, CDCl₃) δ 173.3, 147.7, 139.0, 127.72, 127.49, 56.2, 45.0, 38.6, 36.9, 29.7, 23.0, 11.1 ppm. **ESI-MS**: *m/z* 297.2 [M+H]⁺. **HR-MS**: *m/z* calc. for C₁₄H₂₀N₂O₃S [M+H]⁺: 296.1195; found 296.1198. **HPLC** (PP gradient, MeOH): 4.64 min.

4.1.4.9. *N*-isopropyl-4-(1-methyl-5-oxopyrrolidin-3-yl)benzenesulfonamide (**7i**)

Acquired 46.6 mg (68%) as a white solid from 40.5 mg of **5** using 2-propylamine as the amine (Mobile phase: 2% MeOH in CH₂Cl₂). **¹H NMR** (400 MHz, CDCl₃) δ 7.84 (d, *J* = 8.5 Hz, 2H), 7.35 (d, *J* = 8.2 Hz, 2H), 4.62 (d, *J* = 7.5 Hz, 1H), 3.79 (dd, *J* = 9.7, 8.3 Hz, 1H), 3.65 (dt, *J* = 16.7, 8.2 Hz, 1H), 3.52 – 3.37 (m, 2H), 2.92 (s, 3H), 2.86 (dd, *J* = 17.0, 9.2 Hz, 1H), 2.53 (dd, *J* = 16.9, 7.8 Hz, 1H), 1.08 (d, *J* = 6.5 Hz, 6H) ppm. **¹³C NMR** (101 MHz, CDCl₃) δ 173.3, 147.6, 140.1, 127.66, 127.44, 56.2, 46.2, 38.5, 36.9, 29.7, 23.8 ppm. **ESI-**

MS: m/z 297.2 $[M+H]^+$. **HR-MS:** m/z calc. for $C_{14}H_{20}N_2O_3S$ $[M+H]^+$: 296.1195; found 296.1198. **HPLC** (PP gradient, MeOH): 4.54 min.

4.1.4.10. 8-((4-(1-methyl-5-oxopyrrolidin-3-yl)phenyl)sulfonyl)-8-azabicyclo[3.2.1]octan-3-one (**7j**)

Acquired 28.2 mg (34%) as a white solid from 40.5 mg of **5** using 8-azabicyclo[3.2.1]octan-3-one as the amine (Mobile phase: 2% MeOH in CH_2Cl_2). **1H NMR** (400 MHz, $CDCl_3$) δ 7.87 (d, $J = 8.5$ Hz, 2H), 7.37 (d, $J = 8.3$ Hz, 2H), 4.53 – 4.44 (m, 2H), 3.79 (dd, $J = 9.7, 8.3$ Hz, 1H), 3.65 (dt, $J = 15.9, 8.1$ Hz, 1H), 3.39 (dd, $J = 9.8, 6.5$ Hz, 1H), 2.91 (s, 3H), 2.86 (dd, $J = 16.9, 9.2$ Hz, 1H), 2.78 (dd, $J = 16.0, 4.4$ Hz, 2H), 2.50 (dd, $J = 16.8, 7.7$ Hz, 1H), 2.36 (dd, $J = 16.4, 1.3$ Hz, 2H), 1.75 (dd, $J = 9.2, 4.4$ Hz, 2H), 1.64 – 1.57 (m, 2H) ppm. **^{13}C NMR** (101 MHz, $CDCl_3$) δ 206.7, 173.1, 148.5, 138.7, 127.98, 127.67, 56.12, 56.04, 50.1, 38.5, 36.9, 29.67, 29.42 ppm. **ESI-MS:** m/z 362.9 $[M+H]^+$. **HR-MS:** m/z calc. for $C_{18}H_{22}N_2O_4S$ $[M+H]^+$: 362.1300; found 362.1306. **HPLC** (PP gradient, MeOH): 4.55 min.

4.1.4.11. (3*R*)-1-((4-(1-methyl-5-oxopyrrolidin-3-yl)phenyl)sulfonyl)piperidine-3-carboxylic acid (**7k**)

Acquired 21.4 mg (25%) as a white solid from 40.5 mg of **5** using (*R*)-nipecotic acid as the amine (Reverse-phase HPLC). **1H NMR** (400 MHz, DMSO) δ 7.70 (d, $J = 8.4$ Hz, 2H), 7.57 (d, $J = 8.4$ Hz, 2H), 3.78 – 3.65 (m, 2H), 3.52 (d, $J = 7.0$ Hz, 1H), 3.37 (ddd, $J = 8.8, 6.5, 2.3$ Hz, 2H), 2.77 (s, 3H), 2.69 (dd, $J = 16.5, 8.6$ Hz, 1H), 2.54 – 2.49 (m, 2H), 2.44 – 2.35 (m, 2H), 1.83 – 1.75 (m, 1H), 1.75 – 1.64 (m, 1H), 1.56 – 1.42 (m, 1H), 1.42 – 1.27 (m, 1H) ppm. **^{13}C NMR** (101 MHz, DMSO) δ 173.8, 172.5, 148.5 (d, $J = 3.7$ Hz), 133.8, 128.10, 127.83, 55.0 (d, $J = 2.0$ Hz), 47.5, 46.0, 40.1, 38.0 (d, $J = 3.8$ Hz), 36.5 (d, $J = 1.8$ Hz), 29.1, 25.6, 23.4 ppm. **ESI-MS:** m/z 366.8 $[M+H]^+$. **HR-MS:** m/z calc. for $C_{17}H_{22}N_2O_5S$ $[M+H]^+$: 366.1249; found 366.1250. **HPLC** (PP gradient, 1:1 $CH_3CN:H_2O$): 4.63 min.

^aCompound was extracted from 5% HCl (pH 0).

4.1.4.12. (3*S*)-1-((4-(1-methyl-5-oxopyrrolidin-3-yl)phenyl)sulfonyl)piperidine-3-carboxylic acid (**7l**)

Acquired 17.8 mg (21%) as a white solid from 40.8 mg of **5** using (*S*)-nipecotic acid as the amine (Reverse-phase HPLC). ¹H NMR (400 MHz, DMSO) δ 7.70 (d, *J* = 8.4 Hz, 2H), 7.58 (d, *J* = 8.4 Hz, 2H), 3.80 – 3.65 (m, 2H), 3.53 (d, *J* = 7.0 Hz, 1H), 3.40 – 3.35 (m, 2H), 2.78 (s, 3H), 2.70 (dd, *J* = 16.5, 8.6 Hz, 1H), 2.55 – 2.50 (m, 2H), 2.46 – 2.36 (m, 2H), 1.85 – 1.76 (m, 1H), 1.71 (dd, *J* = 9.0, 4.4 Hz, 1H), 1.57 – 1.43 (m, 1H), 1.43 – 1.29 (m, 1H) ppm. ¹³C NMR (101 MHz, DMSO) δ 173.8, 172.4, 148.5 (d, *J* = 3.7 Hz), 133.7, 128.08, 127.81, 55.0 (d, *J* = 2.1 Hz), 47.5, 46.0, 40.1, 38.0 (d, *J* = 3.9 Hz), 36.5 (d, *J* = 1.9 Hz), 29.1, 25.6, 23.4 ppm. ESI-MS: *m/z* 366.9 [M+H]⁺. HR-MS: *m/z* calc. for C₁₇H₂₂N₂O₅S [M+H]⁺: 366.1249; found 366.1250. HPLC (PP gradient, 1:1 CH₃CN:H₂O): 4.63 min.

^aCompound was extracted from 5% HCl (pH 0).

4.1.4.13. *N*-(3-(1*H*-imidazol-1-yl)propyl)-4-(1-methyl-5-oxopyrrolidin-3-yl)benzenesulfonamide (**7m**)

Acquired 13.2 mg (21%) as a white solid from 30.9 mg of **5** using 3-(1*H*-imidazol-1-yl)propan-1-amine as the amine (Reverse-phase HPLC). ¹H NMR (400 MHz, MeOD) δ 8.84 (s, 1H), 7.80 (d, *J* = 8.5 Hz, 2H), 7.61 (s, 1H), 7.54 (s, 1H), 7.50 (d, *J* = 8.3 Hz, 2H), 4.36 (t, *J* = 6.8 Hz, 2H), 3.86 (dd, *J* = 9.8, 8.3 Hz, 1H), 3.75 (dt, *J* = 16.2, 8.2 Hz, 1H), 3.49 (dd, *J* = 9.8, 6.6 Hz, 1H), 2.90 (s, 3H), 2.89 – 2.80 (m, 3H), 2.51 (dd, *J* = 16.8, 7.9 Hz, 1H), 2.11 – 2.02 (m, 2H) ppm. ¹³C NMR (101 MHz, MeOD) δ 174.6, 148.0, 138.6, 135.5, 127.51, 127.17, 121.7, 120.5, 55.9, 46.0, 39.1, 38.3, 36.8, 29.6, 28.4 ppm. ESI-MS: *m/z* 362.9 [M+H]⁺. HR-MS: *m/z* calc. for C₁₇H₂₂N₄O₃S [M+H]⁺: 362.1413; found 362.1425. HPLC (PP gradient, 1:1 CH₃CN:H₂O): 3.49 min.

4.1.4.14. *N*-(adamantan-1-yl)-4-(1-methyl-5-oxopyrrolidin-3-yl)benzenesulfonamide (**7n**)

Acquired 26.4 mg (38%) as a white solid from 31.4 mg of **5** using adamantan-1-amine as the amine (Mobile phase: 1% MeOH in CH₂Cl₂). **¹H NMR** (400 MHz, CDCl₃) δ 7.86 (d, *J* = 8.5 Hz, 2H), 7.32 (d, *J* = 8.3 Hz, 2H), 4.82 (s, 1H), 3.79 (dd, *J* = 9.7, 8.3 Hz, 1H), 3.70 – 3.59 (m, 1H), 3.41 (dd, *J* = 9.7, 6.6 Hz, 1H), 2.91 (s, 3H), 2.86 (dd, *J* = 17.1, 9.3 Hz, 1H), 2.54 (dd, *J* = 16.8, 7.8 Hz, 1H), 2.00 (br s, 3H), 1.78 (br d, *J* = 2.8 Hz, 6H), 1.57 (br q, *J* = 12.4 Hz, 6H) ppm. **¹³C NMR** (101 MHz, CDCl₃) δ 173.5, 147.2, 143.0, 127.60, 127.34, 56.3, 43.2, 38.6, 37.0, 35.9, 29.78, 29.57 ppm. **ESI-MS**: *m/z* 389.0 [M+H]⁺. **HR-MS**: *m/z* calc. for C₂₁H₂₈N₂O₃S [M+H]⁺: 388.1821; found 388.1828. **HPLC** (PP gradient, MeOH): 6.34 min.

4.1.5. Bromination (NaBr)

1-methyl-4-phenylpyrrolidin-2-one **5** (560 mg, 3.23 mmol) was weighed into a 25 mL round-bottom flask with a stir-bar. NaBr (864 mg, 8.40 mmol) and H₂SO₄ (824 mg, 8.40 mmol) were added and the mixture was heated to 80 °C. It was then stirred for 2 hours or until the dark brown colour disappeared from the walls of the flask. The mixture was cooled to room temperature before being diluted in water (40 mL) and washed with EtOAc (3 x 40 mL). The combined organic layers were dried, filtered and concentrated under reduced pressure to obtain a brown oil. The crude material was checked in analytical HPLC for completion, and was repeated until the starting material was completely consumed. The oil was then purified using column chromatography (Mobile phase: 20% petroleum benzene in EtOAc) to afford bromides **8** and **9**.

4.1.5.1. 4-(2-bromophenyl)-1-methylpyrrolidin-2-one (**8**)

Acquire 112 mg (14%) as a yellow oil. **¹H NMR** (400 MHz, CDCl₃) δ 7.57 (dd, *J* = 8.0, 1.2 Hz, 1H), 7.34 – 7.28 (m, 1H), 7.27 – 7.24 (m, 1H), 7.12 (ddd, *J* = 8.0, 7.2, 1.9 Hz, 1H), 4.07 – 3.96 (m, 1H), 3.82 (dd, *J* = 9.9, 8.2 Hz, 1H), 3.33 (dd, *J* = 9.9, 5.5 Hz, 1H), 2.91 – 2.78 (m, 4H), 2.54 (dd, *J* = 17.0, 6.5 Hz, 1H) ppm. **¹³C NMR** (101 MHz, CDCl₃) δ 173.7, 141.7,

133.3, 128.66, 128.16, 127.1, 124.5, 55.6, 37.6, 36.1, 29.7 ppm. **ESI-MS**: m/z 253.9 [^{79}Br]M+H $^+$ and 255.9 [^{81}Br]M+H $^+$. **HR-MS**: m/z calc. for $\text{C}_{11}\text{H}_{12}\text{BrNO}$ [M+H] $^+$: 253.0102; found 253.0100. **HPLC** (PP gradient, MeOH): 5.70 min.

4.1.5.2. 4-(4-bromophenyl)-1-methylpyrrolidin-2-one (**9**)

Acquired 184 mg (23%) as a clear oil. **^1H NMR** (400 MHz, CDCl_3) δ 7.45 (d, $J = 8.5$ Hz, 2H), 7.09 (d, $J = 8.3$ Hz, 2H), 3.74 (dd, $J = 9.7, 8.3$ Hz, 1H), 3.53 (dt, $J = 16.6, 8.3$ Hz, 1H), 3.35 (dd, $J = 9.7, 6.8$ Hz, 1H), 2.90 (s, 3H), 2.81 (dd, $J = 16.9, 9.1$ Hz, 1H), 2.48 (dd, $J = 16.9, 8.0$ Hz, 1H) ppm. **^{13}C NMR** (101 MHz, CDCl_3) δ 173.7, 141.7, 132.1, 128.6, 121.0, 56.6, 38.8, 36.8, 29.7 ppm. **ESI-MS**: m/z 253.9 [^{79}Br]M+H $^+$ and 255.9 [^{81}Br]M+H $^+$. **HR-MS**: m/z calc. for $\text{C}_{11}\text{H}_{12}\text{BrNO}$ [M+H] $^+$: 253.0102; found 253.0099. **HPLC** (PP gradient, MeOH): 5.90 min.

4.1.6. Bromination (NBS)

N,N-diethyl-4-(1-methyl-5-oxopyrrolidin-3-yl)benzenesulfonamide **9a** (630 mg, 2.03 mmol) was weighed in a round-bottom flask, to which *N*-bromosuccinimide (434 mg, 2.44 mmol) was added, as well as a magnetic stir-bar. Concentrated sulfuric acid (4 mL) was then added, the mixture was heated to 60 °C and the contents were left to stir overnight. After this time, the mixture was quenched with water (50 mL) and washed with EtOAc (3 x 50 mL). The organic layers were combined, dried with MgSO_4 , filtered and concentrated under reduced pressure to give **12** as an oil. This was then purified with column chromatography (Mobile phase: neat EtOAc) to give the bromide **12**.

4.1.6.1. 3-bromo-*N,N*-diethyl-4-(1-methyl-5-oxopyrrolidin-3-yl)benzenesulfonamide (**12**)

Acquired 550 mg (69%) as a purple oil. **^1H NMR** (400 MHz, CDCl_3) δ 8.01 (d, $J = 1.9$ Hz, 1H), 7.72 (dd, $J = 8.2, 1.9$ Hz, 1H), 7.36 (d, $J = 8.2$ Hz, 1H), 4.06 (tt, $J = 8.7, 5.7$ Hz, 1H),

3.86 (dd, $J = 10.2, 8.2$ Hz, 1H), 3.34 (dd, $J = 10.2, 5.2$ Hz, 1H), 3.24 (q, $J = 7.2$ Hz, 4H), 2.95 – 2.85 (m, 4H), 2.54 (dd, $J = 17.3, 5.9$ Hz, 1H), 1.15 (t, $J = 7.1$ Hz, 6H) ppm. ^{13}C NMR (101 MHz, CDCl_3) δ 173.5, 146.1, 140.9, 131.7, 127.7, 126.6, 124.9, 55.3, 42.4, 37.4, 36.2, 29.9, 14.40 ppm. **ESI-MS**: m/z 388.7 [^{79}Br]M+H $^+$ and 390.8 [^{81}Br]M+H $^+$. **HR-MS**: m/z calc. for $\text{C}_{15}\text{H}_{21}\text{BrN}_2\text{O}_3\text{S}$ [M+H] $^+$: 388.0456; found 388.0459. **HPLC** (PP gradient, 1:1 $\text{CH}_3\text{CN}:\text{H}_2\text{O}$): 5.85 min.

4.1.7. Suzuki Coupling

The appropriate bromide was weighed and dissolved in 1,2-dimethoxyethane (5 mL). Upon addition of each reagent, N_2 was bubbled through the mixture for 5 minutes. The appropriate boronic acid (1.2 mol. eq.) was added, followed by 2 M Na_2CO_3 (5 mL) and then $\text{Pd}(\text{PPh}_3)_4$ (3 mol%). After addition of $\text{Pd}(\text{PPh}_3)_4$, the mixture was bubbled with N_2 for 10 minutes before being sealed under a nitrogen atmosphere. The mixture was heated under reflux and left to stir overnight. After this time, the mixture was quenched with saturated aqueous NaCl (25 mL) and washed with EtOAc (3 x 25 mL). The organic layers were combined, dried with MgSO_4 , filtered and concentrated under reduced pressure. The crude products was then purified accordingly to afford the respective products.

4.1.7.1. 4-([1,1'-biphenyl]-2-yl)-1-methylpyrrolidin-2-one (**10**)

Acquired 53.7 mg (70%) as a white solid from 76.5 mg of **8** using phenylboronic acid as the boronic acid (Mobile phase: 40% petroleum benzene in EtOAc). ^1H NMR (400 MHz, CDCl_3) δ 7.47 – 7.35 (m, 5H), 7.32 – 7.22 (m, 4H), 3.72 – 3.60 (m, 1H), 3.52 (dd, $J = 9.7, 8.5$ Hz, 1H), 3.40 (dd, $J = 9.7, 6.8$ Hz, 1H), 2.86 (s, 3H), 2.68 (dd, $J = 16.9, 9.5$ Hz, 1H), 2.54 (dd, $J = 17.0, 7.9$ Hz, 1H) ppm. ^{13}C NMR (101 MHz, CDCl_3) δ 173.9, 142.11, 141.29, 140.58, 130.3, 129.22, 128.42, 128.39, 127.34, 126.67, 125.82, 57.3, 39.9, 33.0, 29.7 ppm. **ESI-MS**: m/z

252.0 [M+H]⁺. **HR-MS**: *m/z* calc. for C₁₇H₁₇NO [M+H]⁺: 251.1310; found 251.1309. **HPLC** (PP gradient, MeOH): 6.46 min.

4.1.7.2. *4-([1,1'-biphenyl]-4-yl)-1-methylpyrrolidin-2-one (11)*

Acquired 44.7 mg (75%) as a white solid from 60.0 mg of **9** using phenylboronic acid as the boronic acid (Mobile phase: 35% petroleum benzene in EtOAc and reverse-phase HPLC). **¹H NMR** (400 MHz, CDCl₃) δ 7.62 – 7.55 (m, 4H), 7.49 – 7.42 (m, 2H), 7.39 – 7.33 (m, 1H), 7.30 (d, *J* = 8.2 Hz, 2H), 3.84 (dd, *J* = 9.8, 8.5 Hz, 1H), 3.74 – 3.63 (m, 1H), 3.52 (dd, *J* = 9.8, 7.0 Hz, 1H), 3.04 – 2.93 (m, 4H), 2.71 (dd, *J* = 17.4, 8.1 Hz, 1H) ppm. **¹³C NMR** (101 MHz, CDCl₃) δ 175.6, 140.89, 140.60, 140.47, 129.0, 127.82, 127.57, 127.26, 127.15, 57.3, 38.7, 37.0, 30.2 ppm. **ESI-MS**: *m/z* 252.0. [M+H]⁺. **HR-MS**: *m/z* calc. for C₁₇H₁₇NO [M+H]⁺: 251.1310; found 251.1310. **HPLC** (PP gradient, 1:1 CH₃CN:H₂O): 6.61 min.

4.1.7.3. *N,N-diethyl-6-(1-methyl-5-oxopyrrolidin-3-yl)-[1,1'-biphenyl]-3-sulfonamide (15a)*

Acquired 10.6 mg (27%) as a clear oil from 40.0 mg of **12** using phenylboronic acid as the boronic acid (Mobile phase: 3% EtOH in Et₂O and reverse-phase HPLC). **¹H NMR** (400 MHz, CDCl₃) δ 7.81 (dd, *J* = 8.3, 2.1 Hz, 1H), 7.69 (d, *J* = 2.0 Hz, 1H), 7.51 – 7.40 (m, 4H), 7.22 (dd, *J* = 7.7, 1.7 Hz, 2H), 3.80 – 3.68 (m, 1H), 3.58 (dd, *J* = 10.1, 8.6 Hz, 1H), 3.42 (dd, *J* = 10.1, 6.5 Hz, 1H), 3.26 (q, *J* = 7.2 Hz, 4H), 2.90 (s, 3H), 2.79 (dd, *J* = 17.3, 9.5 Hz, 1H), 2.61 (dd, *J* = 17.3, 7.5 Hz, 1H), 1.16 (t, *J* = 7.1 Hz, 6H) ppm. **¹³C NMR** (101 MHz, CDCl₃) δ 174.5, 144.8, 143.1, 139.50, 139.08, 129.07, 128.85, 128.83, 128.25, 126.91, 126.70, 57.3, 42.4, 39.5, 33.1, 30.0, 14.5 ppm. **ESI-MS**: *m/z* 386.8 [M+H]⁺. **HR-MS**: *m/z* calc. for C₂₁H₂₆N₂O₃S [M+H]⁺: 386.1664; found 386.1662. **HPLC** (PP gradient, 1:1 CH₃CN:H₂O): 6.33 min.

4.1.7.4. *4'-(dimethylamino)-N,N-diethyl-6-(1-methyl-5-oxopyrrolidin-3-yl)-[1,1'-biphenyl]-3-sulfonamide (15b)*

Acquired 13.1 mg (30%) as a clear oil from 39.6 mg of **12** using (4-(dimethylamino)phenyl)boronic acid as the boronic acid (Mobile phase: 4% EtOH in Et₂O and reverse-phase HPLC). **¹H NMR** (400 MHz, CDCl₃) δ 7.81 (dd, *J* = 8.3, 2.0 Hz, 1H), 7.65 (d, *J* = 2.0 Hz, 1H), 7.50 (d, *J* = 8.3 Hz, 1H), 7.37 (d, *J* = 8.8 Hz, 2H), 7.29 (d, *J* = 8.8 Hz, 2H), 3.74 – 3.64 (m, 1H), 3.60 (t, *J* = 9.2 Hz, 1H), 3.44 (dd, *J* = 9.9, 6.3 Hz, 1H), 3.25 (q, *J* = 7.1 Hz, 4H), 3.18 (s, 6H), 2.90 (s, 3H), 2.77 (dd, *J* = 17.2, 9.4 Hz, 1H), 2.58 (dd, *J* = 17.2, 7.5 Hz, 1H), 1.16 (t, *J* = 7.1 Hz, 6H) ppm. **¹³C NMR** (101 MHz, CDCl₃) δ 174.2, 145.65, 144.90, 141.7, 139.3, 136.5, 130.8, 128.8, 127.17, 126.97, 118.3, 57.2, 44.5, 42.4, 39.6, 33.1, 30.0, 14.5 ppm. **ESI-MS**: *m/z* 429.9 [M+H]⁺. **HR-MS**: *m/z* calc. for C₂₃H₃₁N₃O₃S [M+H]⁺: 429.2086; found 429.2087. **HPLC** (PP gradient, 1:1 CH₃CN:H₂O): 4.94 min.

4.1.7.5. *N,N-diethyl-3',4'-dimethoxy-6-(1-methyl-5-oxopyrrolidin-3-yl)-[1,1'-biphenyl]-3-sulfonamide (15c)*

Acquired 22.6 mg (50%) as a clear oil from 39.7 mg of **12** using (3,4-dimethoxyphenyl)boronic acid as the boronic acid (Mobile phase: 5% EtOH in Et₂O and reverse-phase HPLC). **¹H NMR** (400 MHz, CDCl₃) δ 7.78 (dd, *J* = 8.3, 2.1 Hz, 1H), 7.69 (d, *J* = 2.0 Hz, 1H), 7.46 (d, *J* = 8.3 Hz, 1H), 6.94 (d, *J* = 8.2 Hz, 1H), 6.76 (dd, *J* = 8.1, 2.0 Hz, 1H), 6.72 (d, *J* = 2.0 Hz, 1H), 3.93 (s, 3H), 3.89 (s, 3H), 3.81 – 3.72 (m, 1H), 3.57 (dd, *J* = 10.0, 8.6 Hz, 1H), 3.40 (dd, *J* = 10.0, 6.4 Hz, 1H), 3.25 (q, *J* = 7.1 Hz, 4H), 2.89 (s, 3H), 2.77 (dd, *J* = 17.2, 9.6 Hz, 1H), 2.57 (dd, *J* = 17.2, 7.5 Hz, 1H), 1.16 (t, *J* = 7.1 Hz, 6H) ppm. **¹³C NMR** (101 MHz, CDCl₃) δ 174.0, 149.09, 149.06, 145.3, 142.8, 138.9, 132.1, 128.8, 126.68, 126.62, 121.5, 112.33, 111.32, 57.17, 56.18, 56.14, 42.4, 39.6, 33.1, 30.0, 14.5 ppm. **ESI-MS**: *m/z* 446.8 [M+H]⁺. **HR-MS**: *m/z* calc. for C₂₃H₃₀N₂O₅S [M+H]⁺: 446.1875; found 446.1880. **HPLC** (PP gradient, 1:1 CH₃CN:H₂O): 5.98 min.

4.1.7.6. 3-(benzo[*b*]thiophen-3-yl)-*N,N*-diethyl-4-(1-methyl-5-oxopyrrolidin-3-yl)benzenesulfonamide (**15d**)

Acquired 24.0 mg (54%) as a clear oil from 39.3 mg of **12** using benzo[*b*]thiophen-3-ylboronic acid as the boronic acid (Mobile phase: 3% EtOH in Et₂O and reverse-phase HPLC). ¹H NMR (400 MHz, CDCl₃) (mixture of atropisomers) δ 7.95 (d, *J* = 8.0 Hz, 1H), 7.89 (dd, *J* = 8.3, 2.1 Hz, 1H), 7.75 (d, *J* = 2.0 Hz, 1H), 7.56 (d, *J* = 8.3 Hz, 1H), 7.46 – 7.39 (m, 1H), 7.39 – 7.32 (m, 2H), 7.30 – 7.24 (m, 1H), 3.65 – 3.30 (m, 3H), 3.27 (q, *J* = 7.2 Hz, 4H), 2.83 (br d, *J* = 8.7 Hz, 3H), 2.77 – 2.44 (m, 2H), 1.15 (t, *J* = 7.1 Hz, 6H) ppm. ¹³C NMR (101 MHz, CDCl₃) (mixture of atropisomers) δ 129.6, 127.64, 126.85, 125.1 (d, *J* = 17.4 Hz), 123.20, 122.24, 57.0 (d, *J* = 67.2 Hz), 42.3, 39.84, 38.75, 33.3 (d, *J* = 19.8 Hz), 29.9, 14.4 ppm. **ESI-MS**: *m/z* 442.8 [M+H]⁺. **HR-MS**: *m/z* calc. for C₂₃H₂₆N₂O₃S₂ [M+H]⁺: 442.1385; found 442.1391. **HPLC** (PP gradient, 1:1 CH₃CN:H₂O): 6.79 min.

4.1.8. Heck Coupling and Alkene Reduction

The appropriate bromide was weighed and dissolved in distilled DMF (1 mL). Upon addition of each reagent, N₂ was bubbled through the mixture for 5 minutes. The appropriate alkene (1.6 mol. eq.) was added, followed by DIPEA (300 μL), P(*o*-tol)₃ (10 mol%) and Pd(OAc)₂ (10 mol%). After addition of Pd(OAc)₂, N₂ was bubbled through the mixture for 5 minutes before being sealed, and then vacuumed and backfilled with N₂ three times. The mixture was heated to 90 °C and left to stir overnight. After this time, the mixture was quenched with saturated aqueous NaCl (25 mL) and washed with EtOAc (3 x 25 mL). The organic layers were combined, dried with MgSO₄, filtered and concentrated under reduced pressure to afford the crude alkenes. These were then purified with column chromatography to afford the respective alkenes (**15**) as intermediates. A three-neck 25 mL round-bottom flask with a stir-bar was purged with N₂, to which palladium on carbon (10% w/w) was added, and submerged in a minimum amount of dichloromethane. The appropriate alkene was dissolved

in ethyl acetate and pipetted into the flask while keeping it under N₂. The flask was purged three more times with N₂, and then purged with H₂ three times, to which the contents were left to stir at room temperature. The progress of the reaction was monitored by NMR. After completion, the flask was purged with N₂ three times and the contents filtered carefully through a glass microfiber filter paper under very gentle vacuum. The filtered palladium catalyst was washed with dichloromethane then quenched separately with H₂O while the filtrate was concentrated under reduced pressure to give each reduced product, which were then purified with reverse-phase HPLC.

4.1.8.1. *N,N*-diethyl-4-(1-methyl-5-oxopyrrolidin-3-yl)-3-phenethylbenzenesulfonamide (**14a**)

Acquired 27.7 mg (43%) as a clear oil from 59.7 mg of **12** using styrene as the alkene. ¹H NMR (400 MHz, CDCl₃) δ 7.63 (dd, *J* = 8.2, 2.0 Hz, 1H), 7.59 (d, *J* = 2.0 Hz, 1H), 7.30 (d, *J* = 8.2 Hz, 1H), 7.28 – 7.23 (m, 2H), 7.22 – 7.17 (m, 1H), 7.08 – 7.02 (m, 2H), 3.76 – 3.66 (m, 1H), 3.54 (dd, *J* = 10.2, 8.5 Hz, 1H), 3.26 (dd, *J* = 10.2, 6.0 Hz, 1H), 3.16 (q, *J* = 7.1 Hz, 4H), 3.05 – 2.99 (m, 2H), 2.97 – 2.85 (m, 5H), 2.75 (dd, *J* = 17.3, 9.4 Hz, 1H), 2.45 (dd, *J* = 17.4, 7.0 Hz, 1H), 1.12 (t, *J* = 7.1 Hz, 6H) ppm. ¹³C NMR (101 MHz, CDCl₃) δ 174.5, 145.5, 140.31, 140.27, 139.0, 128.72, 128.65, 128.58, 126.56, 126.44, 125.76, 56.9, 42.3, 39.0, 37.7, 34.7, 32.1, 30.0, 14.4 ppm. **ESI-MS**: *m/z* 414.9 [M+H]⁺. **HR-MS**: *m/z* calc. for C₂₃H₃₀N₂O₃S [M+H]⁺: 414.1977; found 414.1981. **HPLC** (PP gradient, 1:1 CH₃CN:H₂O): 6.62 min.

4.1.8.2. *N,N*-diethyl-4-(1-methyl-5-oxopyrrolidin-3-yl)-3-(3-phenylpropyl)benzenesulfonamide (**14b**)

Acquired 27.3 mg (41%) as a clear oil from 59.9 mg of **12** using allylbenzene as the alkene. ¹H NMR (400 MHz, CDCl₃) δ 7.64 – 7.60 (m, 2H), 7.34 – 7.28 (m, 3H), 7.24 – 7.20 (m, 1H), 7.20 – 7.16 (m, 2H), 3.69 – 3.59 (m, 2H), 3.36 – 3.31 (m, 1H), 3.22 (q, *J* = 7.2 Hz, 4H), 2.92 (s, 3H), 2.84 – 2.76 (m, 1H), 2.73 – 2.65 (m, 4H), 2.49 (dd, *J* = 17.0, 6.4 Hz, 1H), 1.93 – 1.84

(m, 2H), 1.13 (t, $J = 7.1$ Hz, 6H) ppm. ^{13}C NMR (101 MHz, CDCl_3) δ 174.2, 145.2, 141.44, 141.26, 139.1, 128.65, 128.55, 128.30, 126.49, 126.33, 125.60, 56.8, 42.2, 39.0, 35.7, 33.14, 32.43, 31.98, 30.0, 14.37 ppm. **ESI-MS**: m/z 428.9 $[\text{M}+\text{H}]^+$. **HR-MS**: m/z calc. for $\text{C}_{24}\text{H}_{32}\text{N}_2\text{O}_3\text{S}$ $[\text{M}+\text{H}]^+$: 428.2134; found 428.2140. **HPLC** (PP gradient, 1:1 $\text{CH}_3\text{CN}:\text{H}_2\text{O}$): 6.92 min.

4.1.9. Diastereomer Resolution

A 100 mL oven-dried round-bottom flask with a magnetic stir-bar was purged with N_2 . Diisopropylamine (138 mg, 193 μL , 1.37 mmol) was added via syringe and dissolved in distilled THF (5 mL). The contents were stirred, then placed on a dry ice-bath. While kept at -78 $^\circ\text{C}$, *n*-butyllithium (850 μL , 1.37 mmol, 1.6 M in hexane) was then added via syringe and the contents were stirred for 20 minutes. A solution of 4-phenylpyrrolidin-2-one **4** (200 mg, 1.24 mmol) dissolved in distilled THF (10 mL) was added to the mixture via syringe and left to stir for 45 minutes. After this time, (*S*)-Naproxen chloride **16** (617 mg, 2.48 mmol) was dissolved in distilled THF (10 mL) and added via syringe. The contents were lifted off the dry ice-bath and allowed to stir at room temperature for 2.5 hours. Saturated aqueous NaHCO_3 (30 mL) was used to quench the mixture, which was then washed with dichloromethane (3 x 30 mL). The organic layers were combined, dried with MgSO_4 , filtered and concentrated under reduced pressure to afford the crude diastereomers as a solid. The diastereomers were separated using column chromatography (Mobile phase: 10% EtOAc in petroleum benzine, TLCs were checked in 20% EtOAc in petroleum benzine) to afford both (*R,S*)-**17** and (*S,S*)-**17**.

4.1.9.1. (*R*)-1-((*S*)-2-(6-methoxynaphthalen-2-yl)propanoyl)-4-phenylpyrrolidin-2-one ((*R,S*)-**17**)[41]

Acquired 136 mg (29%) as a clear oil. ^1H NMR (400 MHz, CDCl_3) δ 7.73 – 7.70 (m, 3H), 7.49 (dd, $J = 8.5, 1.8$ Hz, 1H), 7.38 – 7.32 (m, 2H), 7.31 – 7.27 (m, 1H), 7.23 – 7.17 (m, 2H),

7.15 – 7.11 (m, 2H), 5.24 (q, $J = 7.0$ Hz, 1H), 4.20 (dd, $J = 11.7, 8.2$ Hz, 1H), 3.80 (dd, $J = 11.7, 8.9$ Hz, 1H), 3.45 – 3.35 (m, 1H), 2.81 (qd, $J = 17.4, 9.3$ Hz, 2H), 1.56 (d, $J = 7.0$ Hz, 3H) ppm. **HPLC** (PP gradient, MeOH): 7.74 min.

4.1.9.2. *(S)-1-((S)-2-(6-methoxynaphthalen-2-yl)propanoyl)-4-phenylpyrrolidin-2-one ((S,S)-17)*[41]

Acquired 136 mg (29%) as a clear oil. $^1\text{H NMR}$ (400 MHz, CDCl_3) δ 7.74 – 7.68 (m, 3H), 7.48 (dd, $J = 8.6, 1.7$ Hz, 1H), 7.20 – 7.12 (m, 4H), 7.12 – 7.06 (m, 2H), 6.98 – 6.92 (m, 2H), 5.24 (q, $J = 7.0$ Hz, 1H), 4.33 (dd, $J = 11.7, 7.9$ Hz, 1H), 3.93 (s, 3H), 3.70 (dd, $J = 11.7, 6.8$ Hz, 1H), 3.56 – 3.43 (m, 1H), 2.94 (dd, $J = 17.5, 8.4$ Hz, 1H), 2.60 (dd, $J = 17.5, 8.0$ Hz, 1H), 1.58 (d, $J = 7.0$ Hz, 3H) ppm. **HPLC** (PP gradient, MeOH): 7.64 min.

4.1.10. *Chiral Auxiliary Uncoupling*

The appropriate imide **17** was weighed in a round-bottom flask, to which a magnetic stir-bar was added. The compound was dissolved in THF and then 1 M KOH was added. The mixture was left to stir overnight. After this time, the organic solvent was evaporated off under reduced pressure, then washed with CH_2Cl_2 (3 x 20 mL). The organic layers were combined, dried with MgSO_4 , filtered and concentrated under reduced pressure to afford the crude lactams. These were purified with column chromatography (Mobile phase: neat EtOAc) to afford each lactam.

4.1.10.1. *(R)-4-phenylpyrrolidin-2-one ((R)-4)*

Acquired 47.1 mg (84%) as a white solid from 134 mg of *(R,S)*-**17**. $[\alpha]_{\text{D}}^{26} - 39.4$ (c 0.9, CHCl_3). $^1\text{H NMR}$ (400 MHz, CDCl_3) δ 7.39 – 7.30 (m, 2H), 7.30 – 7.19 (m, 3H), 7.07 (br s, 1H), 3.83 – 3.74 (m, 1H), 3.68 (dt, $J = 16.9, 8.6$ Hz, 1H), 3.42 (dd, $J = 9.4, 7.2$ Hz, 1H), 2.73 (dd, $J = 16.9, 8.9$ Hz, 1H), 2.51 (dd, $J = 16.9, 8.8$ Hz, 1H) ppm. $^{13}\text{C NMR}$ (101 MHz, CDCl_3) δ 178.1, 142.3, 128.9, 127.17, 126.86, 49.7, 40.4, 38.2 ppm. **ESI-MS**: m/z 162.0 $[\text{M}+\text{H}]^+$.

4.1.10.2. (S)-4-phenylpyrrolidin-2-one ((S)-4)

Acquired 28.4 mg (80%) as a white solid from 81.8 mg of (S,S)-7. $[\alpha]_{\text{D}}^{24} + 44.8$ (c 1, CHCl₃). ¹H NMR (400 MHz, CDCl₃) δ 7.39 – 7.30 (m, 2H), 7.30 – 7.21 (m, 3H), 7.08 (br s, 1H), 3.80 (dd, *J* = 13.2, 4.6 Hz, 1H), 3.69 (dt, *J* = 16.9, 8.6 Hz, 1H), 3.43 (dd, *J* = 9.4, 7.3 Hz, 1H), 2.75 (dd, *J* = 17.0, 8.9 Hz, 1H), 2.53 (dd, *J* = 17.0, 8.8 Hz, 1H) ppm. ¹³C NMR (101 MHz, CDCl₃) δ 178.5, 142.2, 129.0, 127.24, 126.87, 49.8, 40.3, 38.2 ppm. ESI-MS: *m/z* 162.0 [M+H]⁺.

4.1.11. Formation of (R)-15c and (S)-15c

The phenyl NMP isomers (R)-5 and (S)-5 were weighed in separate 10 mL round-bottom flasks and dissolved in CH₂Cl₂ (4 mL). Chlorosulfonic acid (8 mol. eq.) was then slowly pipetted into the mixture at room temperature and left to stir overnight. After this time, the mixture was quenched with water (10 mL) at 0 °C and washed with CH₂Cl₂ (3 x 15 mL). The combined organic layers were dried with MgSO₄, filtered and concentrated under reduced pressure to acquire each sulfonyl chloride as an oil. These were then re-taken up in CH₂Cl₂ (10 mL) and diethylamine (10 mol. eq.) was added, followed by Et₃N (3 mol. eq.) The mixture was left to stir overnight, then the excess amine was evaporated off with rotary evaporation. The residue was quenched in water (10 mL) and washed with CH₂Cl₂ (3 x 15 mL). The organic layers were combined, dried with MgSO₄, filtered and concentrated under reduced pressure to afford each sulfonamide. These were then weighed in separate round-bottom flasks, to which *N*-bromosuccinimide (1.2 mol. eq.) was added, as well as a magnetic stir-bar. Concentrated sulfuric acid (3 mL) was then added, the mixtures were heated to 60 °C and the contents were left to stir overnight. After this time, each mixture was quenched with water (15 mL) and washed with EtOAc (3 x 15 mL). The organic layers were combined, dried with MgSO₄, filtered and concentrated under reduced pressure to give each isomer as an oil. These were then purified with column chromatography (Mobile phase: neat EtOAc) to

give the bromides. Lastly, the bromides were weighed and dissolved in 1,2-dimethoxyethane (5 mL). Upon addition of each reagent, N₂ was bubbled through the mixture for 5 minutes. 3,4-dimethoxyphenylboronic acid (1.2 mol. eq.) was added, followed by 2 M Na₂CO₃ (5 mL) and then Pd(PPh₃)₄ (3 mol%). After addition of Pd(PPh₃)₄, the mixture was bubbled with N₂ for 10 minutes before being sealed under a nitrogen atmosphere. The mixture was heated under reflux and left to stir overnight. After this time, the mixture was quenched with saturated aqueous NaCl (15 mL) and washed with EtOAc (3 x 15 mL). The organic layers were combined, dried with MgSO₄, filtered and concentrated under reduced pressure. The crude products was then purified with column chromatography (Mobile phase: 8% EtOH in Et₂O) to afford the respective isomers.

4.1.11.1. (R)-N,N-diethyl-3',4'-dimethoxy-6-(1-methyl-5-oxopyrrolidin-3-yl)-[1,1'-biphenyl]-3-sulfonamide ((R)-**15c**)

Acquired 5.60 mg (10%) as a clear oil from 22.3 mg of (R)-**5**. **¹H NMR** (400 MHz, CDCl₃) δ 7.78 (dd, *J* = 8.3, 2.0 Hz, 1H), 7.70 (d, *J* = 2.0 Hz, 1H), 7.47 (d, *J* = 8.3 Hz, 1H), 6.94 (d, *J* = 8.2 Hz, 1H), 6.77 (dd, *J* = 8.1, 2.0 Hz, 1H), 6.73 (d, *J* = 2.0 Hz, 1H), 3.94 (s, 3H), 3.89 (s, 3H), 3.79 – 3.69 (m, 1H), 3.55 (dd, *J* = 9.9, 8.5 Hz, 1H), 3.38 (dd, *J* = 9.9, 6.2 Hz, 1H), 3.26 (q, *J* = 7.1 Hz, 4H), 2.88 (s, 3H), 2.72 (dd, *J* = 17.1, 9.5 Hz, 1H), 2.51 (dd, *J* = 16.9, 7.2 Hz, 1H), 1.16 (t, *J* = 7.1 Hz, 6H) ppm. **¹³C NMR** (101 MHz, CDCl₃) δ 173.3, 149.1, 145.7, 142.8, 140.8, 138.9, 132.2, 128.8, 126.67, 126.64, 121.5, 112.4, 111.3, 56.96, 56.20, 56.17, 42.4, 39.8, 33.0, 29.8, 14.5 ppm. **ESI-MS**: *m/z* 447.2 [M+H]⁺. **HR-MS**: *m/z* calc. for C₂₃H₃₀N₂O₅S [M+H]⁺: 446.1875; found 446.1883. **HPLC** (PP gradient, CH₃CN): 5.91 min. **Chiral HPLC**: 5.88 min.

4.1.11.2. (S)-N,N-diethyl-3',4'-dimethoxy-6-(1-methyl-5-oxopyrrolidin-3-yl)-[1,1'-biphenyl]-3-sulfonamide ((S)-**15c**)

Acquired 2.40 mg (8.4%) as a clear oil from 11.2 mg of (*S*)-**5**. **¹H NMR** (400 MHz, CDCl₃) δ 7.78 (dd, *J* = 8.3, 2.1 Hz, 1H), 7.70 (d, *J* = 2.0 Hz, 1H), 7.47 (d, *J* = 8.3 Hz, 1H), 6.94 (d, *J* = 8.2 Hz, 1H), 6.77 (dd, *J* = 8.1, 2.0 Hz, 1H), 6.73 (d, *J* = 2.0 Hz, 1H), 3.94 (s, 3H), 3.89 (s, 3H), 3.78 – 3.68 (m, 1H), 3.55 (dd, *J* = 9.9, 8.5 Hz, 1H), 3.38 (dd, *J* = 9.9, 6.3 Hz, 1H), 3.26 (q, *J* = 7.1 Hz, 4H), 2.88 (s, 3H), 2.72 (dd, *J* = 16.9, 9.7 Hz, 1H), 2.51 (dd, *J* = 17.0, 7.4 Hz, 1H), 1.16 (t, *J* = 7.1 Hz, 6H) ppm. **¹³C NMR** (101 MHz, CDCl₃) δ 128.8, 126.68, 126.65, 121.5, 112.4, 111.3, 56.97, 56.21, 56.17, 42.4, 39.8, 33.1, 29.8, 14.5 ppm. **ESI-MS**: *m/z* 447.2 [M+H]⁺. **HR-MS**: *m/z* calc. for C₂₃H₃₀N₂O₅S [M+H]⁺: 446.1875; found 446.1886. **HPLC** (PP gradient, CH₃CN): 5.91 min. **Chiral HPLC**: 4.75 min.

4.2. Fluorescence Resonance Energy Transfer Assay

The IC₅₀s were measured using a Fluorescence Resonance Energy Transfer (FRET) assay, which was carried out based on the protocol developed by CisBio Assay, France. The assay consists of a europium (Eu³⁺) cryptate-conjugated antibody attached to glutathione *S*-transferase (GST) fused to BRD4 BD1 (49-170) and Streptavidin-D2 bound to biotin which is attached to a Histone H4 peptide, SGRG-K(Ac)-GG-K(Ac)-GLG-K(Ac)-GGAK(Ac)-RHRKVGG-K (Biotin). Both Streptavidin-D2 and the Eu³⁺ cryptate-conjugated antibody were purchased from CisBio Assays. In the absence of inhibitors, the Histone H4 peptide is bound to BRD4 BD1. When both are in close proximity, a 337 nm laser light activates the Eu³⁺ donor and emits at 620 nm, which causes D2 to fluoresce at 665 nm. In the presence of a ligand, this reaction is interrupted. The assays were performed in 384-well small volume microtiter plates. The serially diluted small molecule inhibitors were added to a buffer mixture with a final concentration of 1% DMSO. The final buffer concentrations were 10 nM of GST-BRD4 BD1, 40 nM of Histone H4 peptide, 5 nM of Eu³⁺ cryptate-conjugated GST-antibody, 6.25 nM Streptavidin-D2, 50 mM Hepes, 50 mM NaCl, 0.5 mM CHAPS, 400 mM KF, 0.01% BSA, pH 7.5. After mixing and incubation at room temperature for at least 1.5

hours, the plates were measured in a PheraStar plate reader (BMG Labtech) (excitation: 337 nm with 10 flashes; emission: 620 and 665 nm).

4.3. Crystallisation and Data Collection

X-ray crystal structures were obtained using a 6-His tagged bromodomain, BRD4 BD1, which was expressed in E.coli and purified using Ni-agarose chromatography. The 6-His tag was then removed by TEV protease digestion. The bromodomain was purified using gel filtration chromatography using a Superdex-75, 16/60 column (GE Healthcare) in a buffer containing 50 mM Hepes pH 7.5, 0.3 M NaCl and 5% glycerol. The concentrated BRD4 BD1 protein (17 mg/ml) was then incubated with 50 mM of the ligand at 4 °C for 16h. The final ligand concentration used in the hanging drop was 5 mM. Crystals were obtained using the hanging drop method in 24-well plates using 1 µl drops of protein and the reservoir solution containing 0.2 M NaNO₃, PEG-3350 (35%) and ethylene glycol (6% v/v) concentrations. This was then flash frozen in liquid nitrogen. All datasets were collected at the Australian Synchrotron on MX1 and MX2 beamlines.[49] Datasets were merged and scaled using *MOSFLM*[50] and *AIMLESS*[51] from the CCP4 suite.[52] 5% of reflections in each dataset were flagged for calculation of R_{free} . A summary of statistics is provided in Supplementary Table S1. Molecular replacement was performed with *Phaser*[53] using a previously solved structure of BRD4 as a search model (PDB: 5DW2). The final structures were obtained after several rounds of manual refinement using *Coot*[54] and refinement with *phenix.refine*.[55]

Acknowledgements

This work was supported by a Research Training Program scholarship from the Monash Institute of Pharmaceutical Sciences and a Cancer Council Victoria Venture Grant. This research was undertaken in part using the MX2 beamline at the Australian Synchrotron, part of ANSTO, and made use of the Australian Cancer Research Foundation (ACRF) detector.

Supplementary Data

Supplementary data relating to this article can be found at _____.

References

- [1] C.W. Murray, D.C. Rees, The rise of fragment-based drug discovery, *Nat Chem*, 1 (2009) 187-192.
- [2] D.A. Erlanson, S.W. Fesik, R.E. Hubbard, W. Jahnke, H. Jhoti, Twenty years on: the impact of fragments on drug discovery, *Nat Rev Drug Discov*, 15 (2016) 605-619.
- [3] I.T. Raheem, J.D. Schreier, J. Fuerst, L. Gantert, E.D. Hostetler, S. Huszar, A. Joshi, M. Kandebo, S.H. Kim, J. Li, B. Ma, G. McGaughey, S. Sharma, W.D. Shipe, J. Uslaner, G.H. Vandever, Y. Yan, J.J. Renger, S.M. Smith, P.J. Coleman, C.D. Cox, Discovery of pyrazolopyrimidine phosphodiesterase 10A inhibitors for the treatment of schizophrenia, *Bioorg Med Chem Lett*, 26 (2016) 126-132.
- [4] D.A. Hay, O. Fedorov, S. Martin, D.C. Singleton, C. Tallant, C. Wells, S. Picaud, M. Philpott, O.P. Monteiro, C.M. Rogers, S.J. Conway, T.P. Rooney, A. Tumber, C. Yapp, P. Filippakopoulos, M.E. Bunnage, S. Muller, S. Knapp, C.J. Schofield, P.E. Brennan, Discovery and optimization of small-molecule ligands for the CBP/p300 bromodomains, *J Am Chem Soc*, 136 (2014) 9308-9319.
- [5] E. Casale, N. Amboldi, M.G. Brasca, D. Caronni, N. Colombo, C. Dalvit, E.R. Felder, G. Fogliatto, A. Galvani, A. Isacchi, P. Polucci, L. Riceputi, F. Sola, C. Visco, F. Zuccotto, F. Casuscelli, Fragment-based hit discovery and structure-based optimization of aminotriazolopyrimidines as novel Hsp90 inhibitors, *Bioorg Med Chem*, 22 (2014) 4135-4150.
- [6] M.G. Simpson, M. Pittelkow, S.P. Watson, J.K. Sanders, Dynamic combinatorial chemistry with hydrazones: libraries incorporating heterocyclic and steroidal motifs, *Org Biomol Chem*, 8 (2010) 1181-1187.
- [7] J. Wloch, R.D. Davies, J. Burton, Cubanes in medicinal chemistry: synthesis of functionalized building blocks, *Org Lett*, 16 (2014) 4094-4097.
- [8] M. Brewer, O. Ichihara, C. Kirchhoff, M. Schade, M. Whittaker, Assembling a Fragment Library, in: *Fragment-Based Drug Discovery*, 2008, pp. 39-62.
- [9] H. Prescher, G. Koch, T. Schuhmann, P. Ertl, A. Bussenault, M. Glick, I. Dix, F. Petersen, D.E. Lizos, Construction of a 3D-shaped, natural product like fragment library by fragmentation and diversification of natural products, *Bioorgan Med Chem*, 25 (2017) 921-925.
- [10] J.A. Johnson, C.A. Nicolaou, S.E. Kirberger, A.K. Pandey, H. Hu, W.C.K. Pomerantz, Evaluating the Advantages of Using 3D-Enriched Fragments for Targeting BET Bromodomains, *ACS Medicinal Chemistry Letters*, 10 (2019) 1648-1654.

- [11] C. Dalvit, S. Knapp, 19F NMR isotropic chemical shift for efficient screening of fluorinated fragments which are racemates and/or display multiple conformers, *Magnetic Resonance in Chemistry*, 55 (2017) 1091-1095.
- [12] Y. Wang, J.-Y. Wach, P. Sheehan, C. Zhong, C. Zhan, R. Harris, S.C. Almo, J. Bishop, S.J. Haggarty, A. Ramek, K.N. Berry, C. O'Herin, A.N. Koehler, A.W. Hung, D.W. Young, Diversity-Oriented Synthesis as a Strategy for Fragment Evolution against GSK3 β , *ACS Medicinal Chemistry Letters*, 7 (2016) 852-856.
- [13] R. Zhang, P.J. McIntyre, P.M. Collins, D.J. Foley, C. Arter, F. von Delft, R. Bayliss, S. Warriner, A. Nelson, Construction of a Shape-Diverse Fragment Set: Design, Synthesis and Screen against Aurora-A Kinase, *Chemistry – A European Journal*, 25 (2019) 6831-6839.
- [14] A.M. Taylor, A. Côté, M.C. Hewitt, R. Pastor, Y. Leblanc, C.G. Nasveschuk, F.A. Romero, T.D. Crawford, N. Cantone, H. Jayaram, J. Setser, J. Murray, M.H. Beresini, G. de Leon Boenig, Z. Chen, A.R. Conery, R.T. Cummings, L.A. Dakin, E.M. Flynn, O.W. Huang, S. Kaufman, P.J. Keller, J.R. Kiefer, T. Lai, Y. Li, J. Liao, W. Liu, H. Lu, E. Pardo, V. Tsui, J. Wang, Y. Wang, Z. Xu, F. Yan, D. Yu, L. Zawadzke, X. Zhu, X. Zhu, R.J. Sims, A.G. Cochran, S. Bellon, J.E. Audia, S. Magnuson, B.K. Albrecht, Fragment-Based Discovery of a Selective and Cell-Active Benzodiazepinone CBP/EP300 Bromodomain Inhibitor (CPI-637), *ACS Medicinal Chemistry Letters*, 7 (2016) 531-536.
- [15] M. Naderi, C. Alvin, Y. Ding, S. Mukhopadhyay, M. Brylinski, A graph-based approach to construct target-focused libraries for virtual screening, *J Cheminform*, 8 (2016) 14.
- [16] D.S. Hewings, M. Wang, M. Philpott, O. Fedorov, S. Uttarkar, P. Filippakopoulos, S. Picaud, C. Vuppusetty, B. Marsden, S. Knapp, S.J. Conway, T.D. Heightman, 3,5-dimethylisoxazoles act as acetyl-lysine-mimetic bromodomain ligands, *J Med Chem*, 54 (2011) 6761-6770.
- [17] M.J. Bennett, Y. Wu, A. Bloor, J. Matuszkiewicz, S.M. O'Connell, L. Shi, R.K. Stansfield, J.R. Del Rosario, J.M. Veal, D.J. Hosfield, J. Xu, S.W. Kaldor, J.A. Stafford, J.M. Betancort, Design, synthesis and biological evaluation of novel 4-phenylisoquinolinone BET bromodomain inhibitors, *Bioorg Med Chem Lett*, 28 (2018) 1811-1816.
- [18] Q. Xiang, C. Wang, Y. Zhang, X. Xue, M. Song, C. Zhang, C. Li, C. Wu, K. Li, X. Hui, Y. Zhou, J.B. Smaill, A.V. Patterson, D. Wu, K. Ding, Y. Xu, Discovery and optimization of 1-(1H-indol-1-yl)ethanone derivatives as CBP/EP300 bromodomain inhibitors for the treatment of castration-resistant prostate cancer, *Eur J Med Chem*, 147 (2018) 238-252.
- [19] G. Lolli, A. Caflisch, High-Throughput Fragment Docking into the BAZ2B Bromodomain: Efficient in Silico Screening for X-Ray Crystallography, *ACS Chem Biol*, 11 (2016) 800-807.
- [20] J. Zhu, A. Caflisch, Twenty Crystal Structures of Bromodomain and PHD Finger Containing Protein 1 (BRPF1)/Ligand Complexes Reveal Conserved Binding Motifs and Rare Interactions, *J Med Chem*, 59 (2016) 5555-5561.
- [21] P.V. Fish, P. Filippakopoulos, G. Bish, P.E. Brennan, M.E. Bunnage, A.S. Cook, O. Federov, B.S. Gerstenberger, H. Jones, S. Knapp, B. Marsden, K. Nocka, D.R. Owen, M. Philpott, S. Picaud, M.J. Primiano, M.J. Ralph, N. Sciammetta, J.D. Trzuppek, Identification

of a chemical probe for bromo and extra C-terminal bromodomain inhibition through optimization of a fragment-derived hit, *J Med Chem*, 55 (2012) 9831-9837.

[22] A.M. Taylor, A. Cote, M.C. Hewitt, R. Pastor, Y. Leblanc, C.G. Nasveschuk, F.A. Romero, T.D. Crawford, N. Cantone, H. Jayaram, J. Setser, J. Murray, M.H. Beresini, G. de Leon Boenig, Z. Chen, A.R. Conery, R.T. Cummings, L.A. Dakin, E.M. Flynn, O.W. Huang, S. Kaufman, P.J. Keller, J.R. Kiefer, T. Lai, Y. Li, J. Liao, W. Liu, H. Lu, E. Pardo, V. Tsui, J. Wang, Y. Wang, Z. Xu, F. Yan, D. Yu, L. Zawadzke, X. Zhu, X. Zhu, R.J. Sims, 3rd, A.G. Cochran, S. Bellon, J.E. Audia, S. Magnuson, B.K. Albrecht, Fragment-Based Discovery of a Selective and Cell-Active Benzodiazepinone CBP/EP300 Bromodomain Inhibitor (CPI-637), *ACS Med Chem Lett*, 7 (2016) 531-536.

[23] R. Sanghvi, R. Narazaki, S.G. Machatha, S.H. Yalkowsky, Solubility improvement of drugs using N-methyl pyrrolidone, *AAPS PharmSciTech*, 9 (2008) 366-376.

[24] M. Philpott, J. Yang, T. Tumber, O. Fedorov, S. Uttarkar, P. Filippakopoulos, S. Picaud, T. Keates, I. Felletar, A. Ciulli, S. Knapp, T.D. Heightman, Bromodomain-peptide displacement assays for interactome mapping and inhibitor discovery, *Mol Biosyst*, 7 (2011) 2899-2908.

[25] J. Shortt, A.K. Hsu, B.P. Martin, K. Doggett, G.M. Matthews, M.A. Doyle, J. Ellul, T.E. Jockel, D.M. Andrews, S.J. Hogg, A. Reitsma, D. Faulkner, P.L. Bergsagel, M. Chesi, J.K. Heath, W.A. Denny, P.E. Thompson, P.J. Neeson, D.S. Ritchie, G.A. McArthur, R.W. Johnstone, The drug vehicle and solvent N-methylpyrrolidone is an immunomodulator and antimyeloma compound, *Cell Rep*, 7 (2014) 1009-1019.

[26] N. Igoe, E.D. Bayle, O. Fedorov, C. Tallant, P. Savitsky, C. Rogers, D.R. Owen, G. Deb, T.C. Somervaille, D.M. Andrews, N. Jones, A. Cheasty, H. Ryder, P.E. Brennan, S. Muller, S. Knapp, P.V. Fish, Design of a Biased Potent Small Molecule Inhibitor of the Bromodomain and PHD Finger-Containing (BRPF) Proteins Suitable for Cellular and in Vivo Studies, *J Med Chem*, 60 (2017) 668-680.

[27] B. Gjoksi, N. Ruangsawasdi, C. Ghayor, B. Siegenthaler, M. Zenobi-Wong, F.E. Weber, Influence of N-methyl pyrrolidone on the activity of the pulp-dentine complex and bone integrity during osteoporosis, *Int Endod J*, 50 (2017) 271-280.

[28] C. Ghayor, R.M. Corroero, K. Lange, L.S. Karfeld-Sulzer, K.W. Gratz, F.E. Weber, Inhibition of osteoclast differentiation and bone resorption by N-methylpyrrolidone, *J Biol Chem*, 286 (2011) 24458-24466.

[29] B. Gjoksi, C. Ghayor, I. Bhattacharya, M. Zenobi-Wong, F.E. Weber, The bromodomain inhibitor N-methyl pyrrolidone reduced fat accumulation in an ovariectomized rat model, *Clinical epigenetics*, 8 (2016) 42.

[30] T.P. Rooney, P. Filippakopoulos, O. Fedorov, S. Picaud, W.A. Cortopassi, D.A. Hay, S. Martin, A. Tumber, C.M. Rogers, M. Philpott, M. Wang, A.L. Thompson, T.D. Heightman, D.C. Pryde, A. Cook, R.S. Paton, S. Muller, S. Knapp, P.E. Brennan, S.J. Conway, A series of potent CREBBP bromodomain ligands reveals an induced-fit pocket stabilized by a cationic interaction, *Angew Chem Int Ed Engl*, 53 (2014) 6126-6130.

- [31] H.G. Ozer, D. El-Gamal, B. Powell, Z.A. Hing, J.S. Blachly, B. Harrington, S. Mitchell, N.R. Grieselhuber, K. Williams, T.H. Lai, L. Alinari, R.A. Baiocchi, L. Brinton, E. Baskin, M. Cannon, L. Beaver, V.M. Goettl, D.M. Lucas, J.A. Woyach, D. Sampath, A.M. Lehman, L. Yu, J. Zhang, Y. Ma, Y. Zhang, W. Spevak, S. Shi, P. Severson, R. Shellooe, H. Carias, G. Tsang, K. Dong, T. Ewing, A. Marimuthu, C. Tantoy, J. Walters, L. Sanftner, H. Rezaei, M. Nespi, B. Matusow, G. Habets, P. Ibrahim, C. Zhang, E.A. Mathe, G. Bollag, J.C. Byrd, R. Lapalombella, BRD4 Profiling Identifies Critical Chronic Lymphocytic Leukemia Oncogenic Circuits and Reveals Sensitivity to PLX51107, a Novel Structurally Distinct BET Inhibitor, *Cancer Discov*, 8 (2018) 458-477.
- [32] P. Bamborough, C.W. Chung, E.H. Demont, R.C. Furze, A.J. Bannister, K.H. Che, H. Diallo, C. Douault, P. Grandi, T. Kouzarides, A.M. Michon, D.J. Mitchell, R.K. Prinjha, C. Rau, S. Robson, R.J. Sheppard, R. Upton, R.J. Watson, A Chemical Probe for the ATAD2 Bromodomain, *Angew Chem Int Ed Engl*, 55 (2016) 11382-11386.
- [33] X. Li, J. Zhang, L. Zhao, Y. Yang, H. Zhang, J. Zhou, Design, Synthesis, and in vitro Biological Evaluation of 3,5-Dimethylisoxazole Derivatives as BRD4 Inhibitors, *ChemMedChem*, 13 (2018) 1363-1368.
- [34] J.P. Hilton-Proctor, O. Ilyichova, Z. Zheng, I.G. Jennings, R.W. Johnstone, J. Shortt, S.J. Mountford, M.J. Scanlon, P.E. Thompson, Synthesis and elaboration of N-methylpyrrolidone as an acetamide fragment substitute in bromodomain inhibition, *Bioorganic & Medicinal Chemistry*, 27 (2019) 115157.
- [35] F. Felluga, V. Gombac, G. Pitacco, E. Valentin, A short and convenient chemoenzymatic synthesis of both enantiomers of 3-phenylGABA and 3-(4-chlorophenyl)GABA (Baclofen), *Tetrahedron: Asymmetry*, 16 (2005) 1341-1345.
- [36] J.P. Day, B. Lindsay, T. Riddell, Z. Jiang, R.W. Allcock, A. Abraham, S. Sookup, F. Christian, J. Bogum, E.K. Martin, R.L. Rae, D. Anthony, G.M. Rosair, D.M. Houslay, E. Huston, G.S. Baillie, E. Klussmann, M.D. Houslay, D.R. Adams, Elucidation of a structural basis for the inhibitor-driven, p62 (SQSTM1)-dependent intracellular redistribution of cAMP phosphodiesterase-4A4 (PDE4A4), *J Med Chem*, 54 (2011) 3331-3347.
- [37] Y.Y. Myint, M.A. Pasha, Oxidative monobromination of electron-rich arenes by conc. H₂SO₄ / alkali metal bromides, *J. Chem. Research*, 2004 (2004) 732-734.
- [38] J.W. Goodby, K.J. Toyne, R.A. Lewis, M. Hird, A.J. Slaney, J.C. Jones, Quinoline 2,6-derivatives as liquid crystal material for display devices, in, the Secretary of State for Defence, UK . 2000, pp. 26 pp.
- [39] K. Rajesh, M. Somasundaram, R. Saiganesh, K.K. Balasubramanian, Bromination of deactivated aromatics: a simple and efficient method, *J Org Chem*, 72 (2007) 5867-5869.
- [40] I.L. Scott, V.A. Kuksa, R. Kubota, Preparation of phenylpropylamine derivatives for treating ophthalmic diseases and disorders, in, Acucela Inc, USA . 2010, pp. 255pp.
- [41] I.J. Montoya-Balbas, B. Valentin-Guevara, E. Lopez-Mendoza, I. Linzaga-Elizalde, M. Ordonez, P. Roman-Bravo, Efficient Synthesis of beta-Aryl-gamma-lactams and Their Resolution with (S)-Naproxen: Preparation of (R)- and (S)-Baclofen, *Molecules*, 20 (2015) 22028-22043.

- [42] R. Gosmini, V.L. Nguyen, J. Toum, C. Simon, J.-M.G. Brusq, G. Krysa, O. Mirguet, A.M. Riou-Eymard, E.V. Boursier, L. Trottet, P. Bamborough, H. Clark, C.-w. Chung, L. Cutler, E.H. Demont, R. Kaur, A.J. Lewis, M.B. Schilling, P.E. Soden, S. Taylor, A.L. Walker, M.D. Walker, R.K. Prinjha, E. Nicodème, The Discovery of I-BET726 (GSK1324726A), a Potent Tetrahydroquinoline ApoA1 Up-Regulator and Selective BET Bromodomain Inhibitor, *Journal of Medicinal Chemistry*, 57 (2014) 8111-8131.
- [43] C.-w. Chung, A.W. Dean, J.M. Woolven, P. Bamborough, Fragment-Based Discovery of Bromodomain Inhibitors Part 1: Inhibitor Binding Modes and Implications for Lead Discovery, *Journal of Medicinal Chemistry*, 55 (2012) 576-586.
- [44] R.P. Law, S.J. Atkinson, P. Bamborough, C.-w. Chung, E.H. Demont, L.J. Gordon, M. Lindon, R.K. Prinjha, A.J.B. Watson, D.J. Hirst, Discovery of Tetrahydroquinoxalines as Bromodomain and Extra-Terminal Domain (BET) Inhibitors with Selectivity for the Second Bromodomain, *Journal of Medicinal Chemistry*, 61 (2018) 4317-4334.
- [45] S.W. Ember, J.Y. Zhu, S.H. Olesen, M.P. Martin, A. Becker, N. Berndt, G.I. Georg, E. Schonbrunn, Acetyl-lysine binding site of bromodomain-containing protein 4 (BRD4) interacts with diverse kinase inhibitors, *ACS Chem Biol*, 9 (2014) 1160-1171.
- [46] Z. Chen, H. Zhang, S. Liu, Y. Xie, H. Jiang, W. Lu, H. Xu, L. Yue, Y. Zhang, H. Ding, M. Zheng, K. Yu, K. Chen, H. Jiang, C. Luo, Discovery of novel trimethoxy-ring BRD4 bromodomain inhibitors: AlphaScreen assay, crystallography and cell-based assay, *Medchemcomm*, 8 (2017) 1322-1331.
- [47] I. Navratilova, T. Aristotelous, S. Picaud, A. Chaikuad, S. Knapp, P. Filappakopoulos, A.L. Hopkins, Discovery of New Bromodomain Scaffolds by Biosensor Fragment Screening, *ACS Med Chem Lett*, 7 (2016) 1213-1218.
- [48] H. Zhao, L. Gartenmann, J. Dong, D. Spiliotopoulos, A. Caflisch, Discovery of BRD4 bromodomain inhibitors by fragment-based high-throughput docking, *Bioorg Med Chem Lett*, 24 (2014) 2493-2496.
- [49] T.M. McPhillips, S.E. McPhillips, H.-J. Chiu, A.E. Cohen, A.M. Deacon, P.J. Ellis, E. Garman, A. Gonzalez, N.K. Sauter, R.P. Phizackerley, Blu-Ice and the Distributed Control System: software for data acquisition and instrument control at macromolecular crystallography beamlines, *Journal of synchrotron radiation*, 9 (2002) 401-406.
- [50] T.G.G. Battye, L. Kontogiannis, O. Johnson, H.R. Powell, A.G.W. Leslie, iMOSFLM: a new graphical interface for diffraction-image processing with MOSFLM, *Acta crystallographica. Section D, Biological crystallography*, 67 (2011) 271-281.
- [51] P.R. Evans, G.N. Murshudov, How good are my data and what is the resolution?, *Acta crystallographica. Section D, Biological crystallography*, 69 (2013) 1204-1214.
- [52] M.D. Winn, C.C. Ballard, K.D. Cowtan, E.J. Dodson, P. Emsley, P.R. Evans, R.M. Keegan, E.B. Krissinel, A.G. Leslie, A. McCoy, S.J. McNicholas, G.N. Murshudov, N.S. Pannu, E.A. Potterton, H.R. Powell, R.J. Read, A. Vagin, K.S. Wilson, Overview of the CCP4 suite and current developments, *Acta Crystallogr D Biol Crystallogr*, 67 (2011) 235-242.

- [53] A.J. McCoy, R.W. Grosse-Kunstleve, P.D. Adams, M.D. Winn, L.C. Storoni, R.J. Read, Phaser crystallographic software, *J Appl Crystallogr*, 40 (2007) 658-674.
- [54] P. Emsley, B. Lohkamp, W.G. Scott, K. Cowtan, Features and development of Coot, *Acta Crystallogr D Biol Crystallogr*, 66 (2010) 486-501.
- [55] P.V. Afonine, R.W. Grosse-Kunstleve, N. Echols, J.J. Headd, N.W. Moriarty, M. Mustyakimov, T.C. Terwilliger, A. Urzhumtsev, P.H. Zwart, P.D. Adams, Towards automated crystallographic structure refinement with phenix.refine, *Acta Crystallogr D Biol Crystallogr*, 68 (2012) 352-367.

Journal Pre-proof

Highlights

Fragment Based Drug Design (FBDD) from the solvent N-methylpyrrolidine (NMP) as BET bromodomain inhibitors.

Successive aromatic substitution reactions to build inhibitors ~200-fold more potent than NMP.

Chiral and Enantiopure synthesis of phenyl-NMP and derivatives.

Crystal structure show pose switch of most potent inhibitor.

Journal Pre-proof

Declaration of interests

The authors declare that they have no known competing financial interests or personal relationships that could have appeared to influence the work reported in this paper.

The authors declare the following financial interests/personal relationships which may be considered as potential competing interests:

Journal Pre-proof